

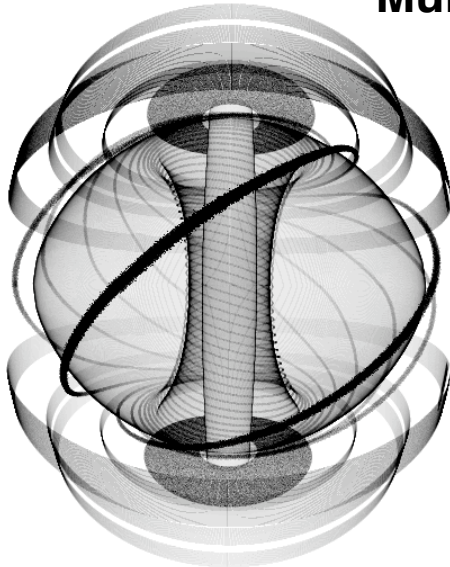
Highlights of the STW03 Workshop

9th Spherical Tokamak Workshop, Culham Science Centre, UK, 15th-17th July 2003

S. S. Medley, NSTX Physics Meeting, 9/29/03

Results from MAST

- Internal Transport Barrier Formation: *Anthony Field*
- SOL and Exhaust Physics: *Glenn Counsell*
- Structure of ELMs: *Andrew Kirk*
- Pellet Injection: *Celso Ribeiro*
- Snake Studies: *Ian Lahane*
- Multichord Zeff Measurements: *Ash Patel*

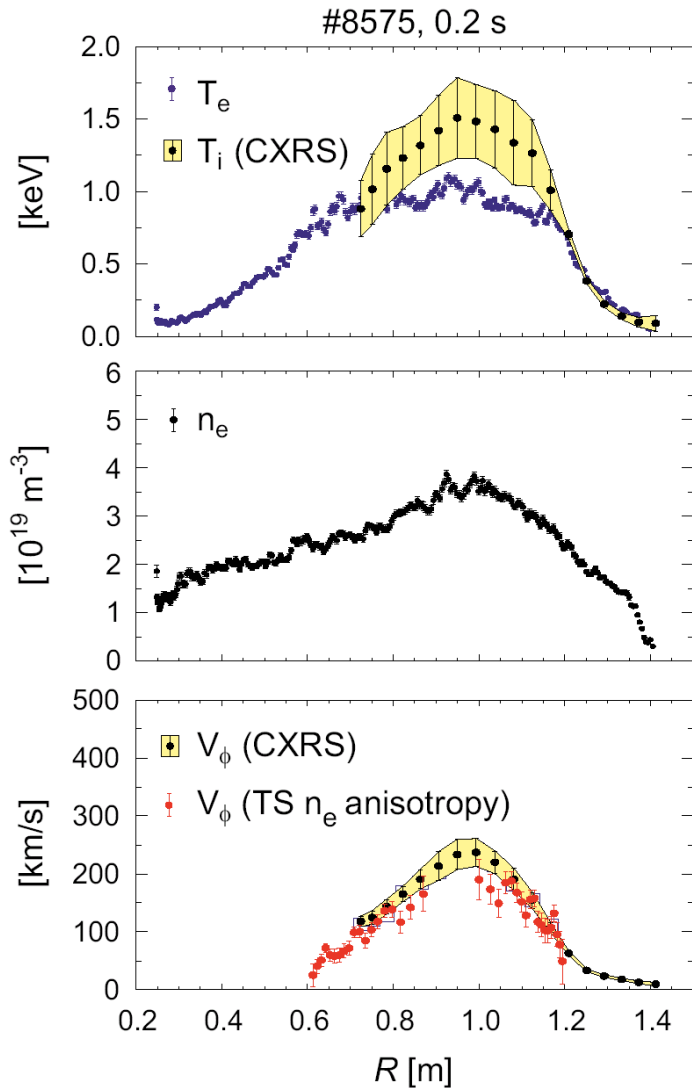


Other Topics

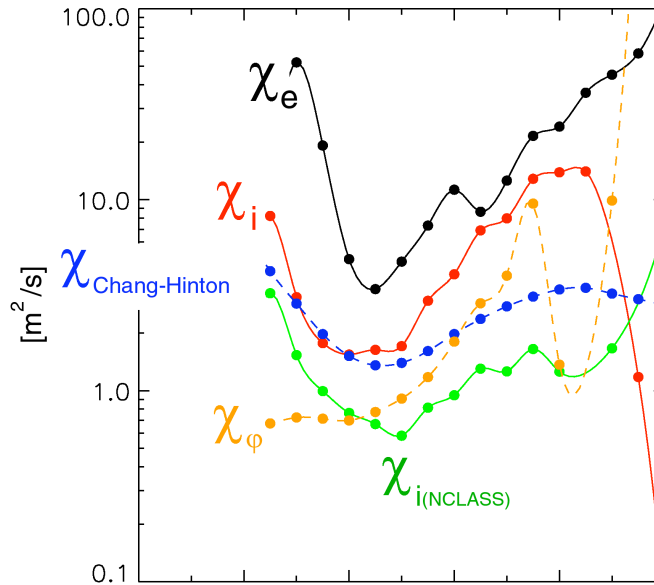
- MAST Facility in 2004: *Alan Sykes*
- EBW CD Start-up Scenario: *A. Saveliev*
- PROTO-SPHERA Proposal: *A. Mancuso*

<http://fusion.org.uk/stw/>

ITBs with co-NBI - early heating, fast I_p ramp



Anthony Field



$\chi_e \sim 3m^2/s$ in the barrier region

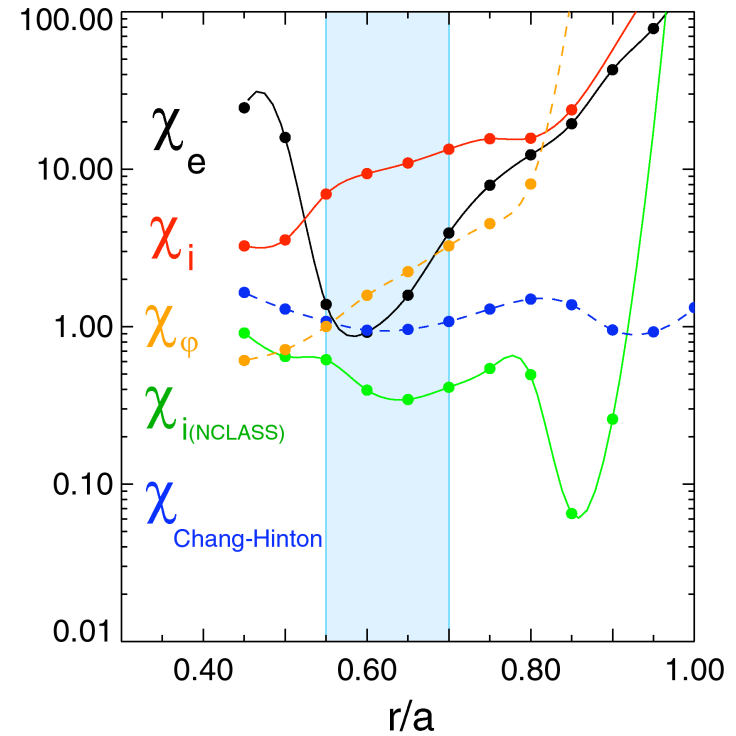
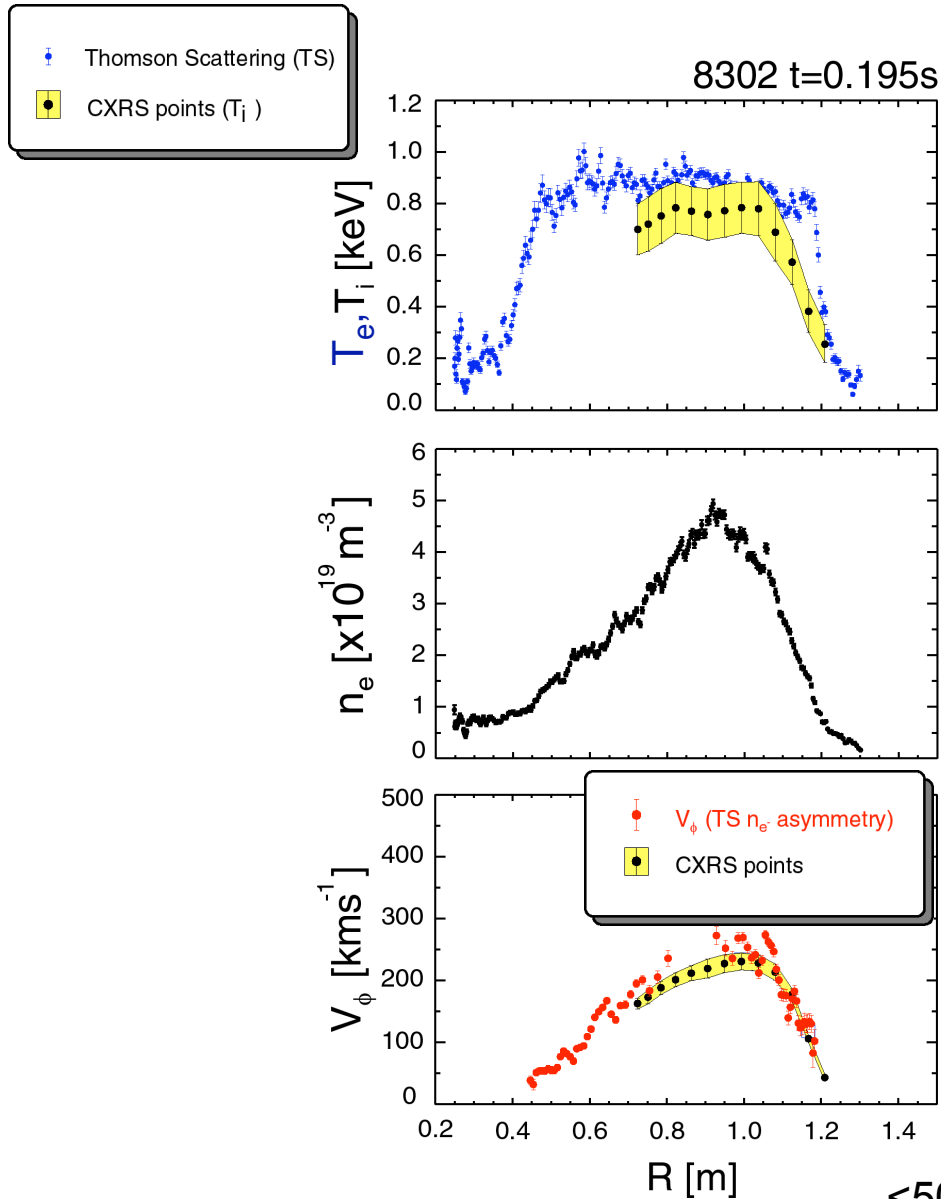
$\chi_i \sim 2m^2/s$ (comparable to Z-corrected Chang Hinton neoclassical value) in the barrier region

$\chi_\phi \sim 0.7m^2/s$ in the barrier region (3x lower than χ_i)

$\chi_e > \chi_i \sim \chi_{CH}$ in the barrier region

$\sim 90\%$ of the NBI power is absorbed by the plasma

Broad, Strong Electron ITB with counter-NBI



$\chi_e \sim 1 \text{ m}^2/\text{s}$ in the barrier region (\sim Chang Hinton χ_i)

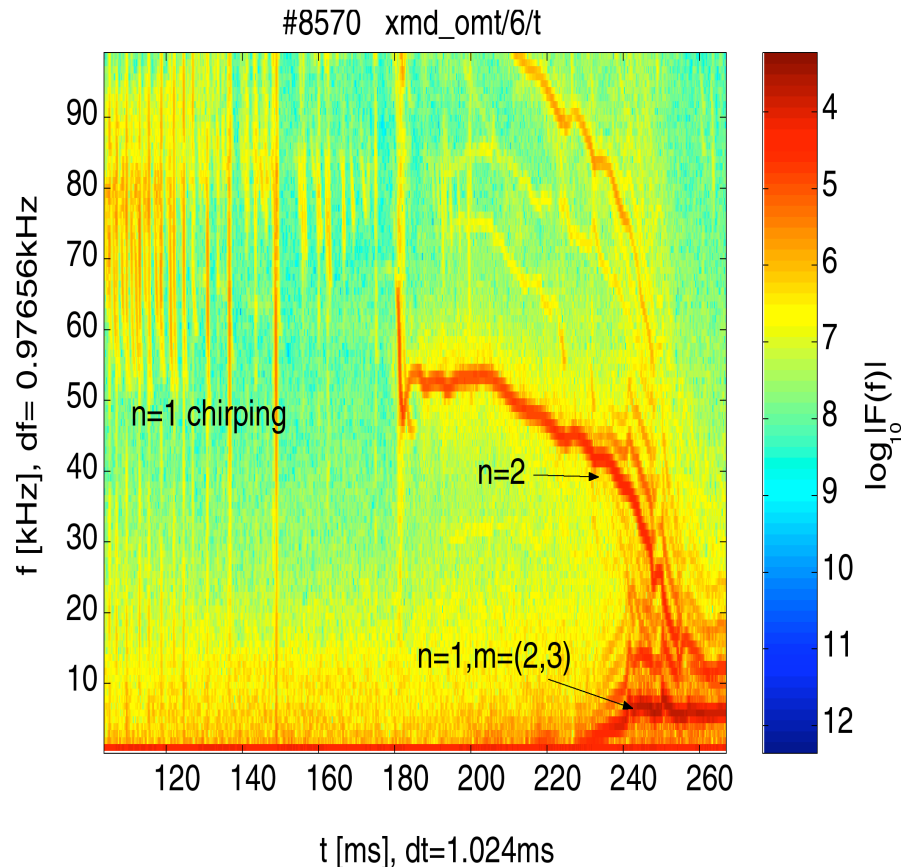
$\chi_i \sim 10 \text{ m}^2/\text{s}$ (no evidence of ion ITB)

$\chi_\phi \sim 2.0 \text{ m}^2/\text{s}$ in the barrier region (5x lower than χ_i)

$\chi_i > \chi_e \sim \chi_{\text{CH}}$ in the barrier region

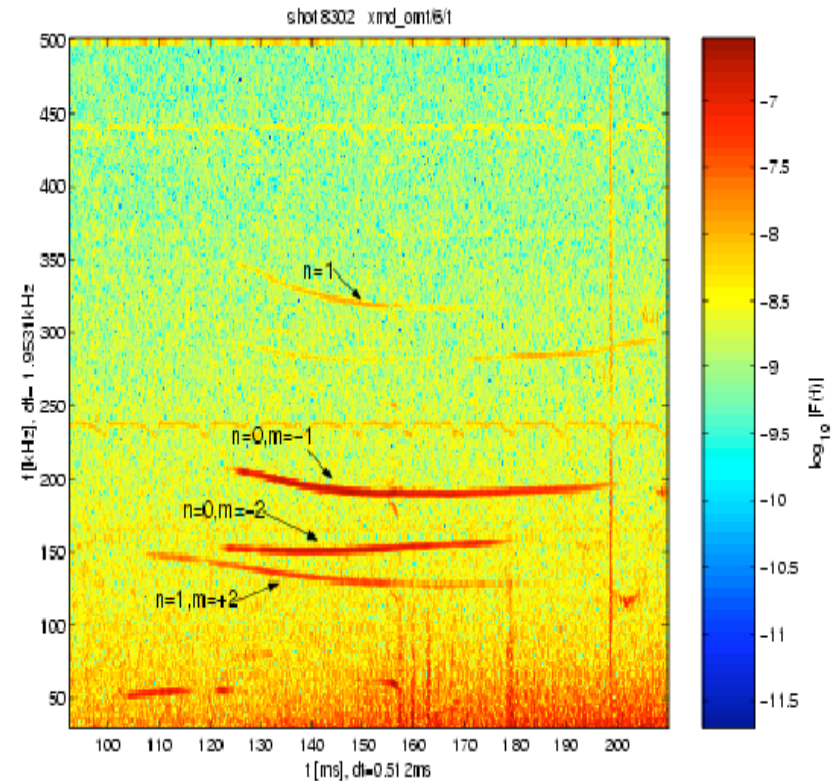
<50% of the NBI power is absorbed by the plasma

Co-NBI: MHD activity ...



- Chirping modes present during I_p ramp
- Low frequency ($\sim 50 \text{ kHz}$) $n=2$ tearing mode couples to $n=1$ mode
- Modes co-exist while NBI is sustained, the driven rotation preventing locking

Counter-NBI: MHD activity ...

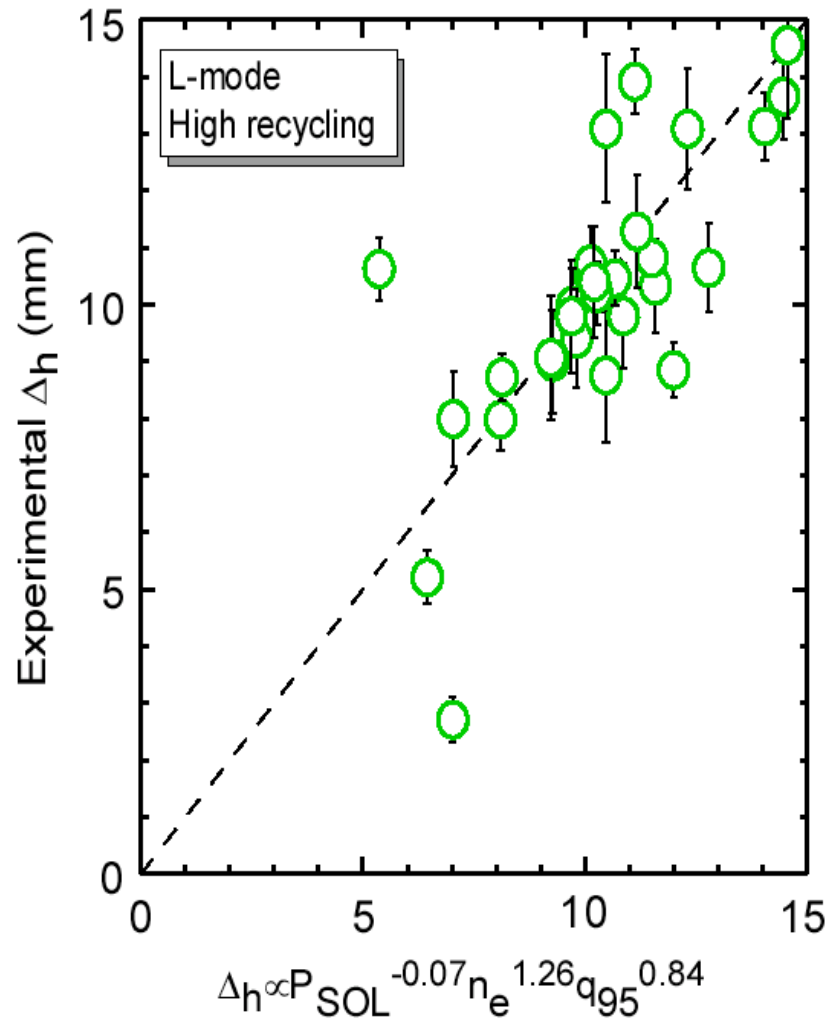


Low-frequency mode activity almost entirely absent

High-frequency $> 150 \text{ kHz}$ $n=0$ modes present throughout

Possibly GAEs driven by 'bump-in-tail' ion distribution due to fast-ion losses

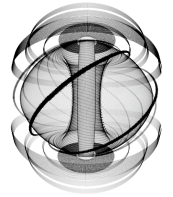
Scalings for L-mode SOL heat flux width developed



- **CDN high recycling regime**
 - weak -ve dependence on P_{SOL}
 - approx. linear with n_e and q_{95}
- **Inner and outer SOL comparison gives robust B_T scaling:**
 - approx. with $1/B_T$

Glenn Counsell

ExB convective cells broaden SOL



- **Toroidally asymmetric biasing**

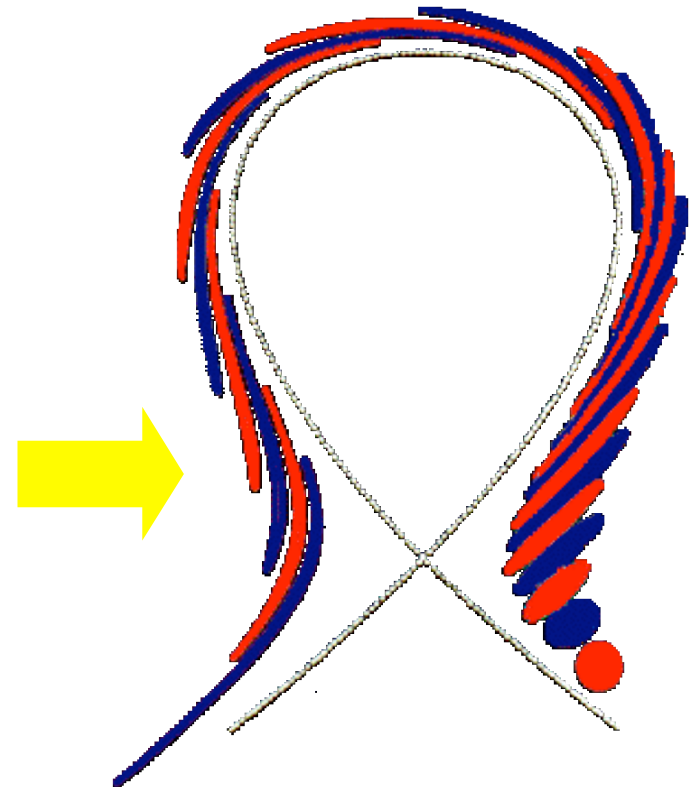
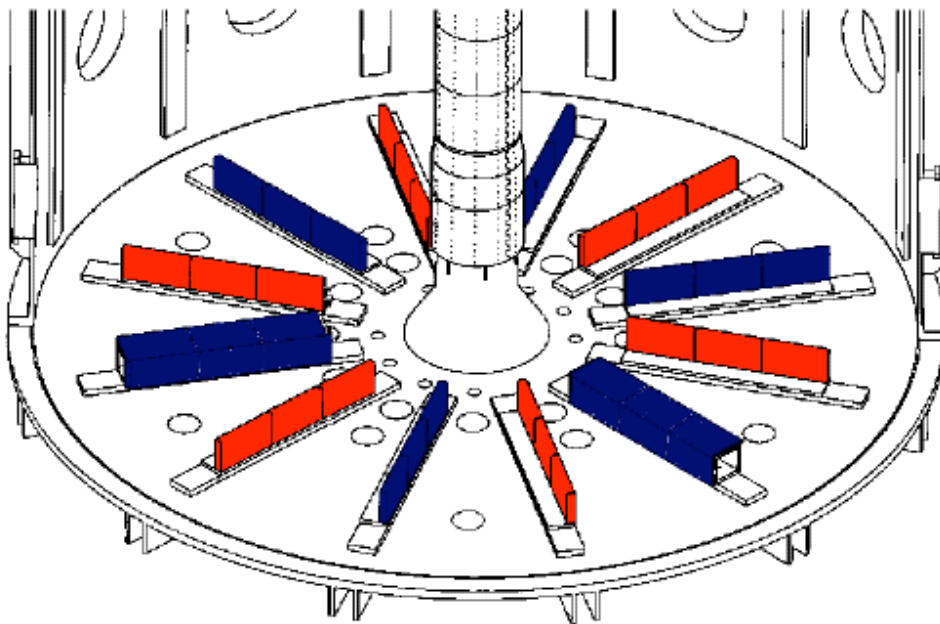
- ⇒ Potential variations in SOL

- ⇒ ExB driven convective cells $v = c \frac{\mathbf{B} \times \nabla \phi}{B^2}$

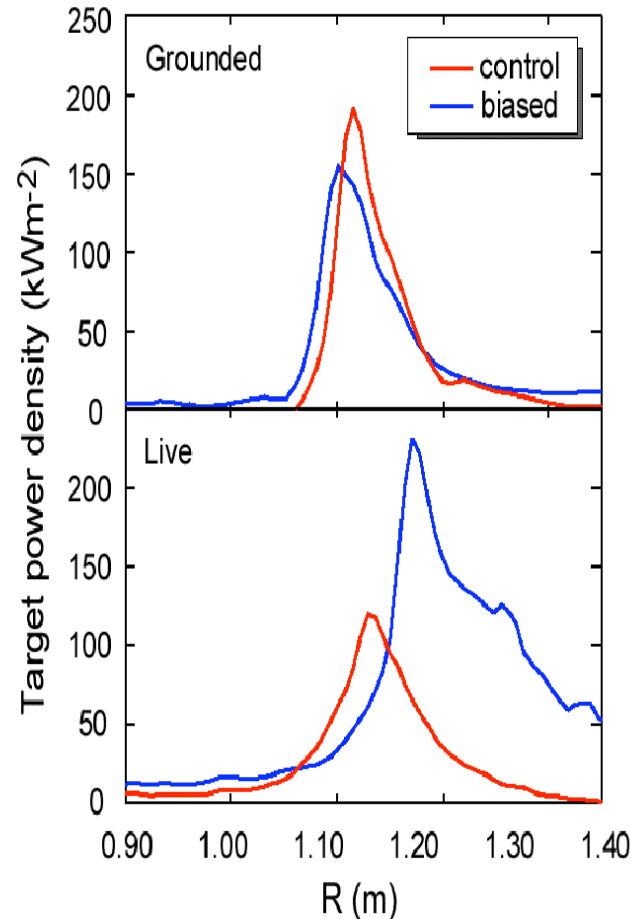
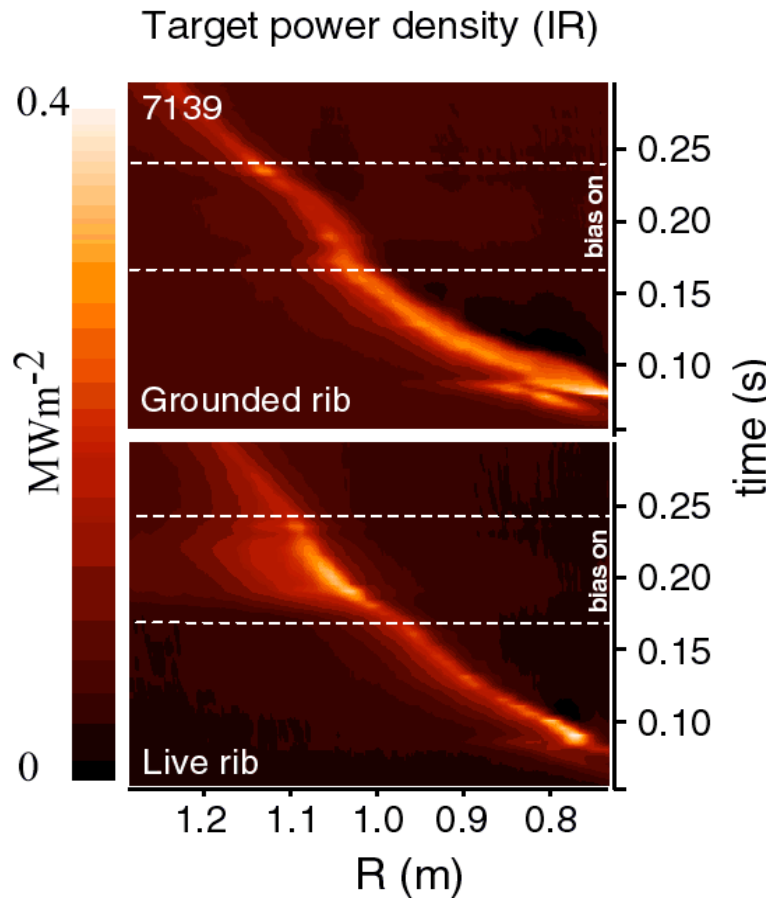
- ⇒ SOL broadening

- ⇒ Reduction of power density

- Applications to ITER using passive, self-biasing of components (different materials, angled tiles etc.)



Divertor biasing - power deposition

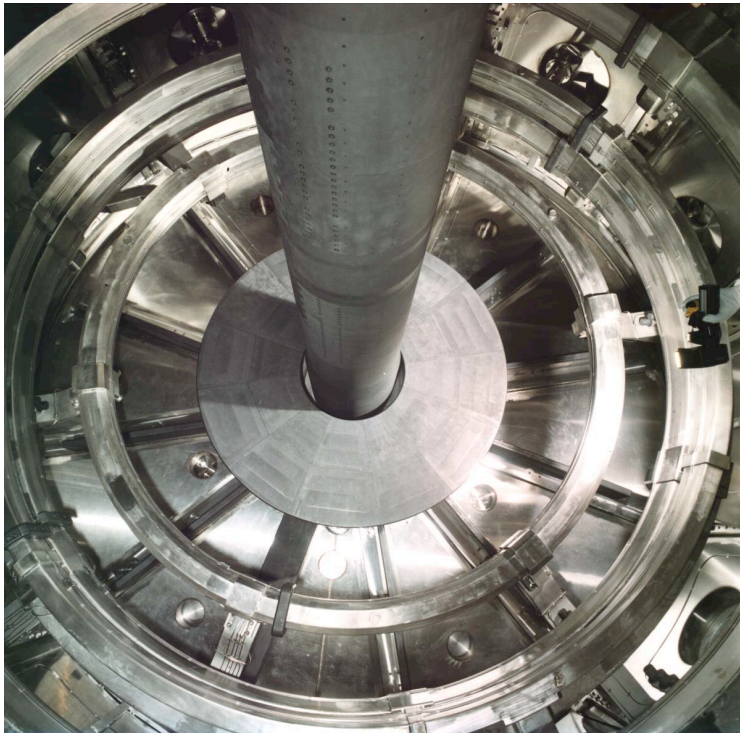


P_{peak} reduced &
slight broadening of
power deposition

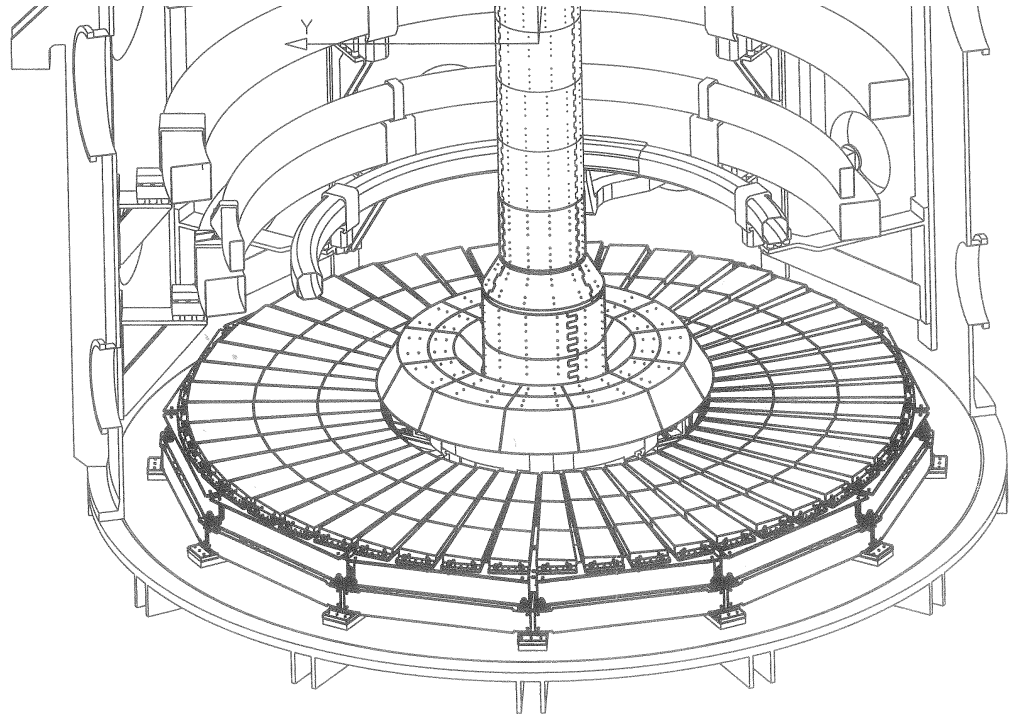
x3 broadening of
power deposition but
 P_{peak} rises
(NB. $P_{\text{bias}}/P_{\square} \sim 0.3$)

ExB drift shifts peak power several cm in opposite directions on live and grounded ribs - explicit prediction of theory

MAST Improved Divertor (MID)



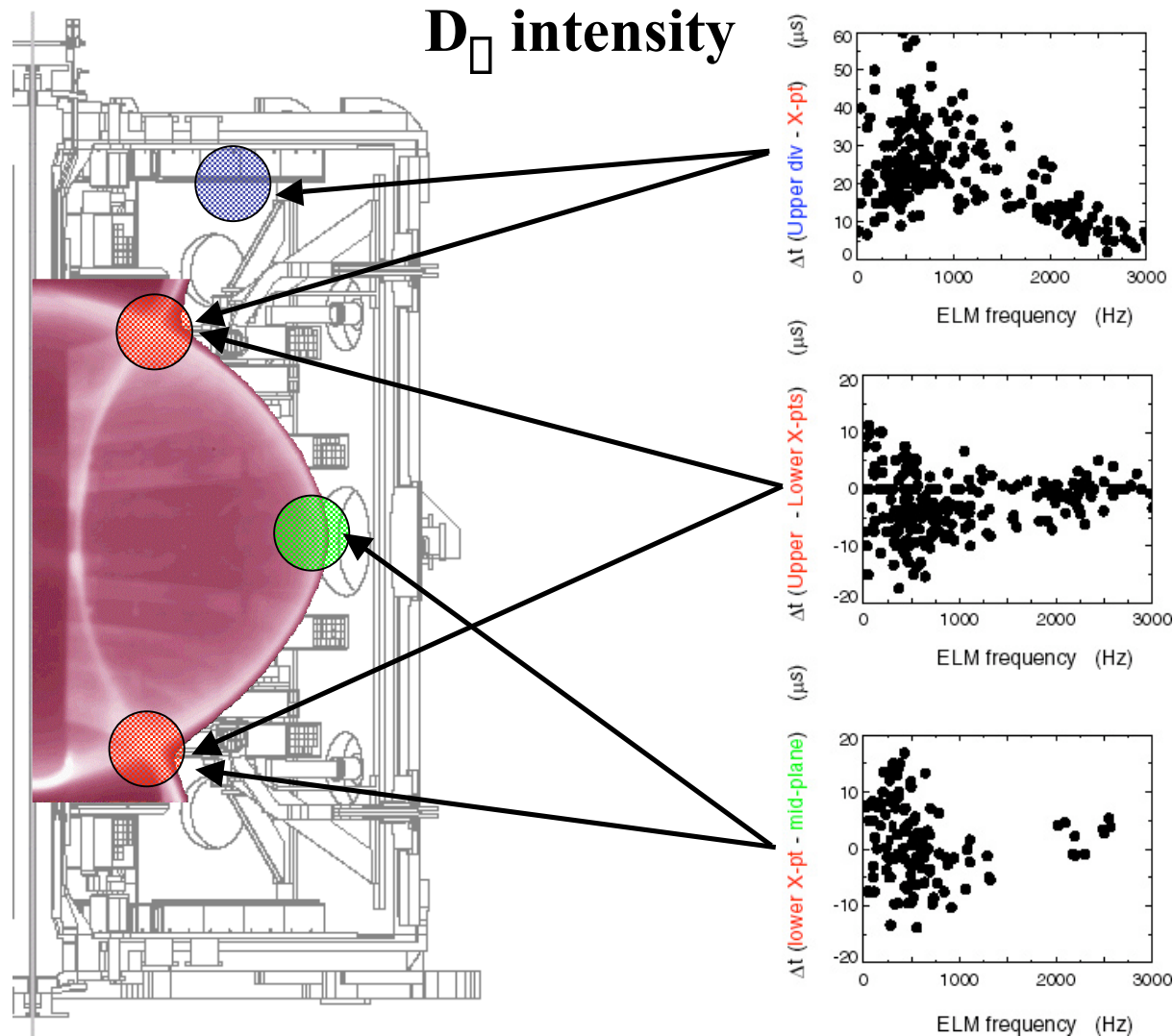
Present divertor
(simple P2 plate, ribs on tank ends)



MID

- Shaped P2 plates
- Imbricated tile divertor plates allow radial biasing
- Improved centre column armour

Poloidal distribution of ELM efflux



Time difference between D_{\square} peak at X-point to target dominated by // transport

No statistically significant time delay between X-points

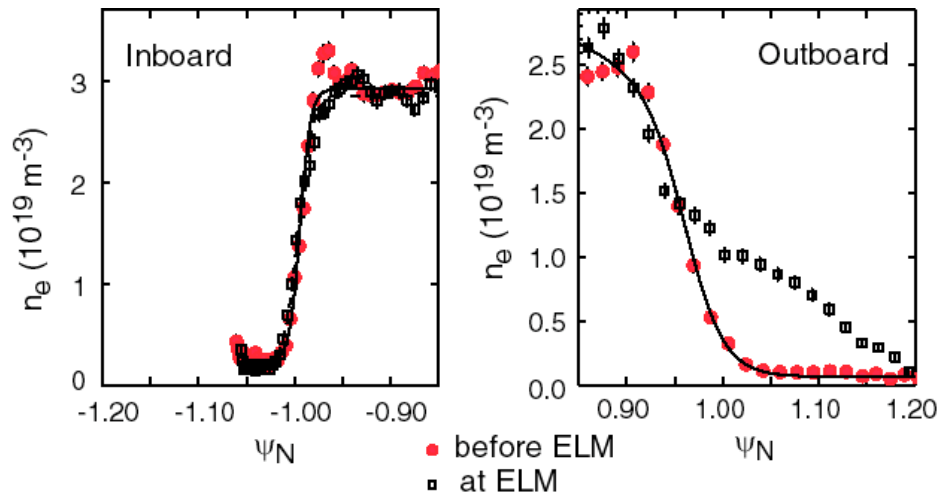
Nor between LFS mid-plane and X-points

Andrew Kirk

D_{\square} and target probe data suggests ELM efflux is released simultaneously at many poloidal locations

ELMs at the mid-plane

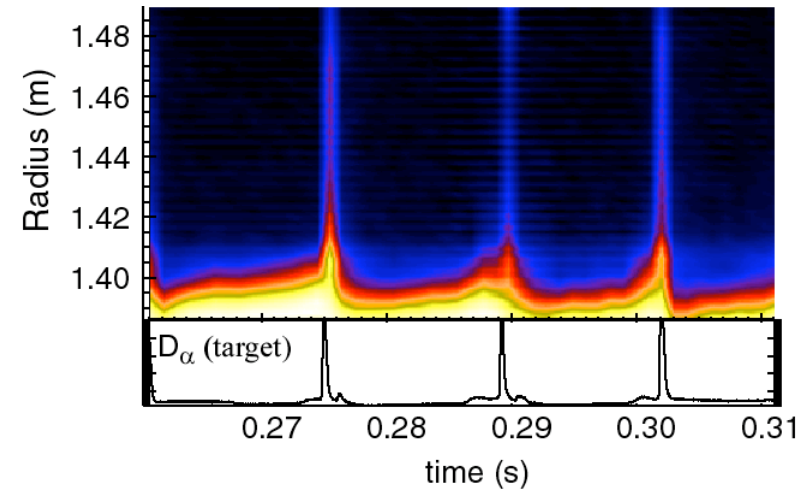
Thomson scattering



Most TS profiles obtained near ELM peak show broad LFS n_e tail

Not observed on the HFS

Linear D_{\square}

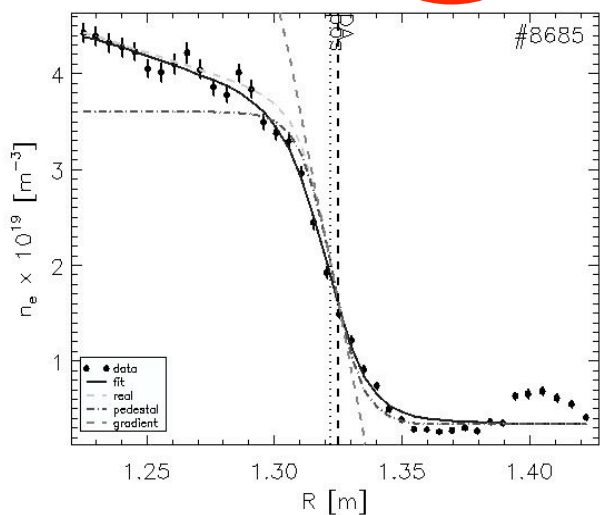
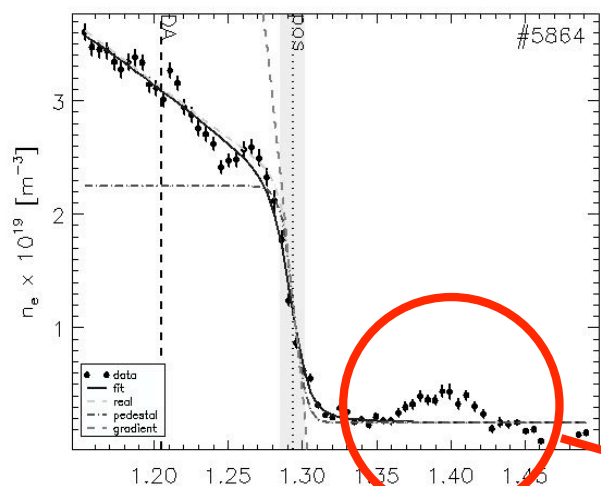


Also seen on mid-plane linear D_{\square} camera

Up to several cm from separatrix

ELMs are characterised by ballooning-like behaviour

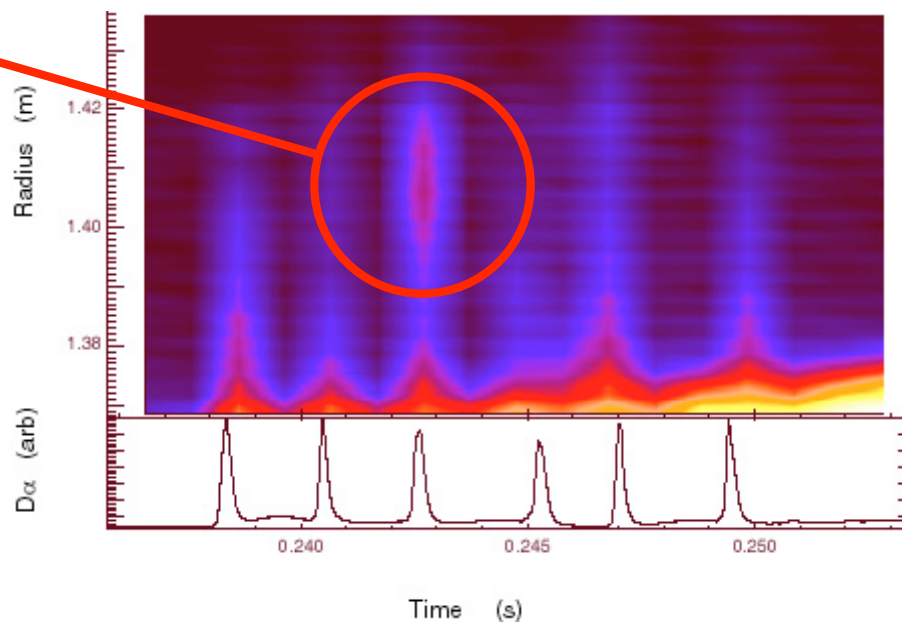
ELM effluxes outside the separatrix



1 in 5 times when Thomson Scattering (TS) fires a “feature” is observed in the n_e and T_e profiles outside the LCFS

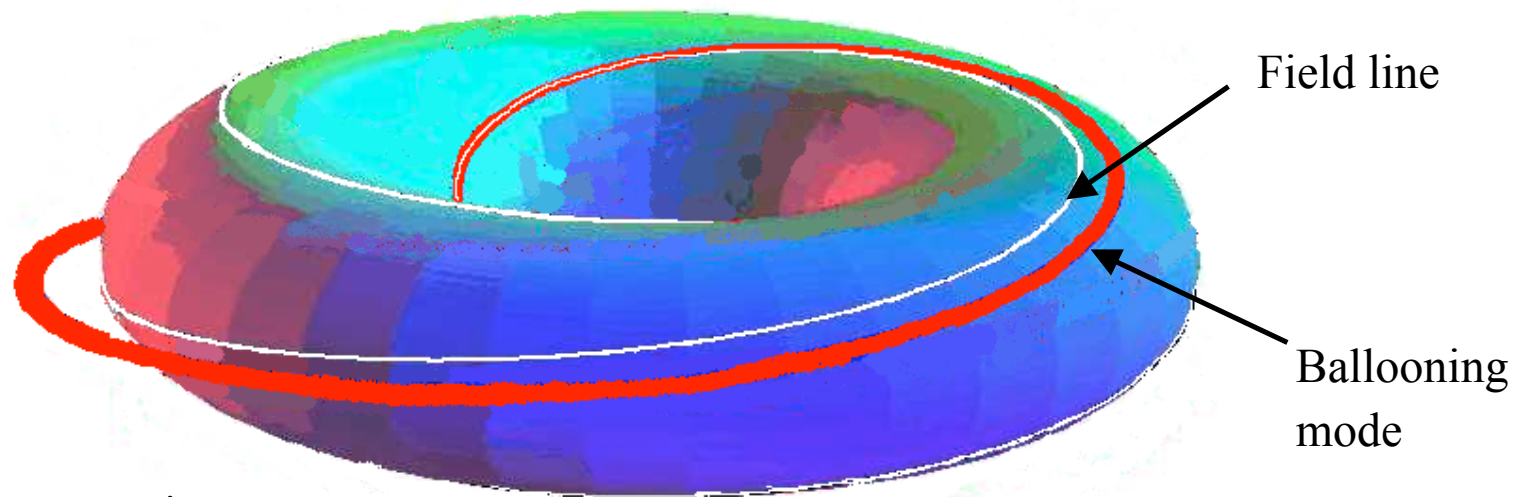
Only observed when TS within 20 μs of an ELM

Also observed on the linear D_α



Non-linear ballooning theory

Work by Cowley and Wilson using non-linear ballooning theory predicts that ELMs may be hot plasma filaments that push out into the SOL

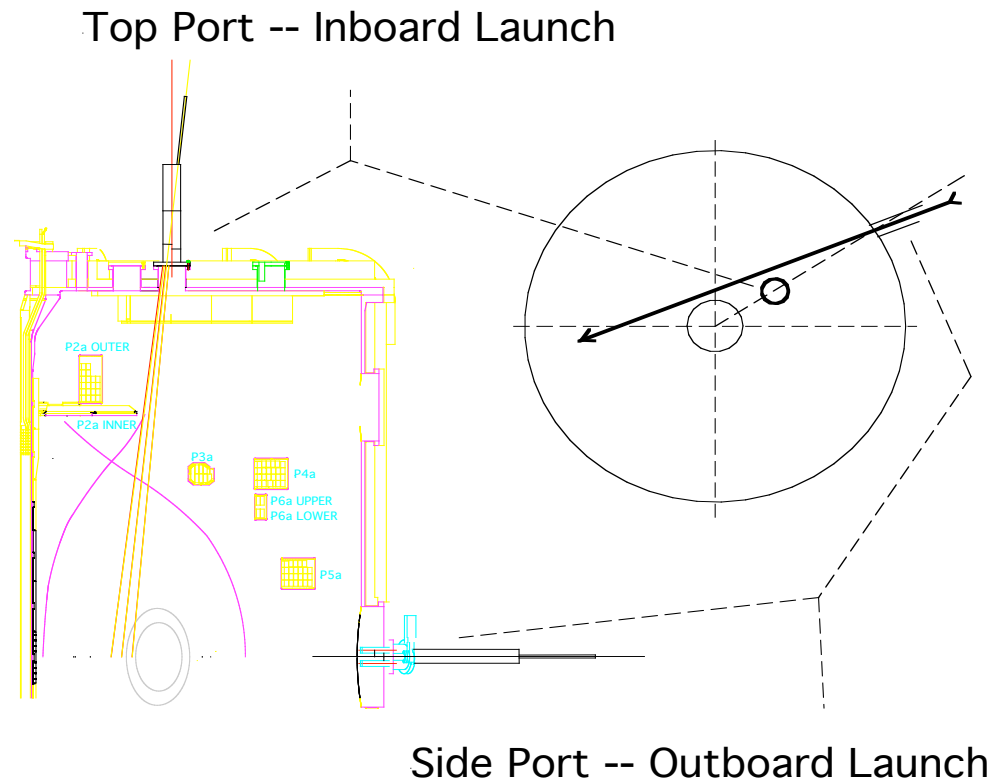


- Mode structure is:
 - elongated along a field line
 - localised in the flux surface, perpendicular to the field line (θ -direction)
 - relatively extended radially (ρ -direction)
- Ballooning mode grows explosively as time approaches a “detonation” time

Pellet Injection Schemes

Pellet Entry into MAST to July 2003

Celso Ribeiro

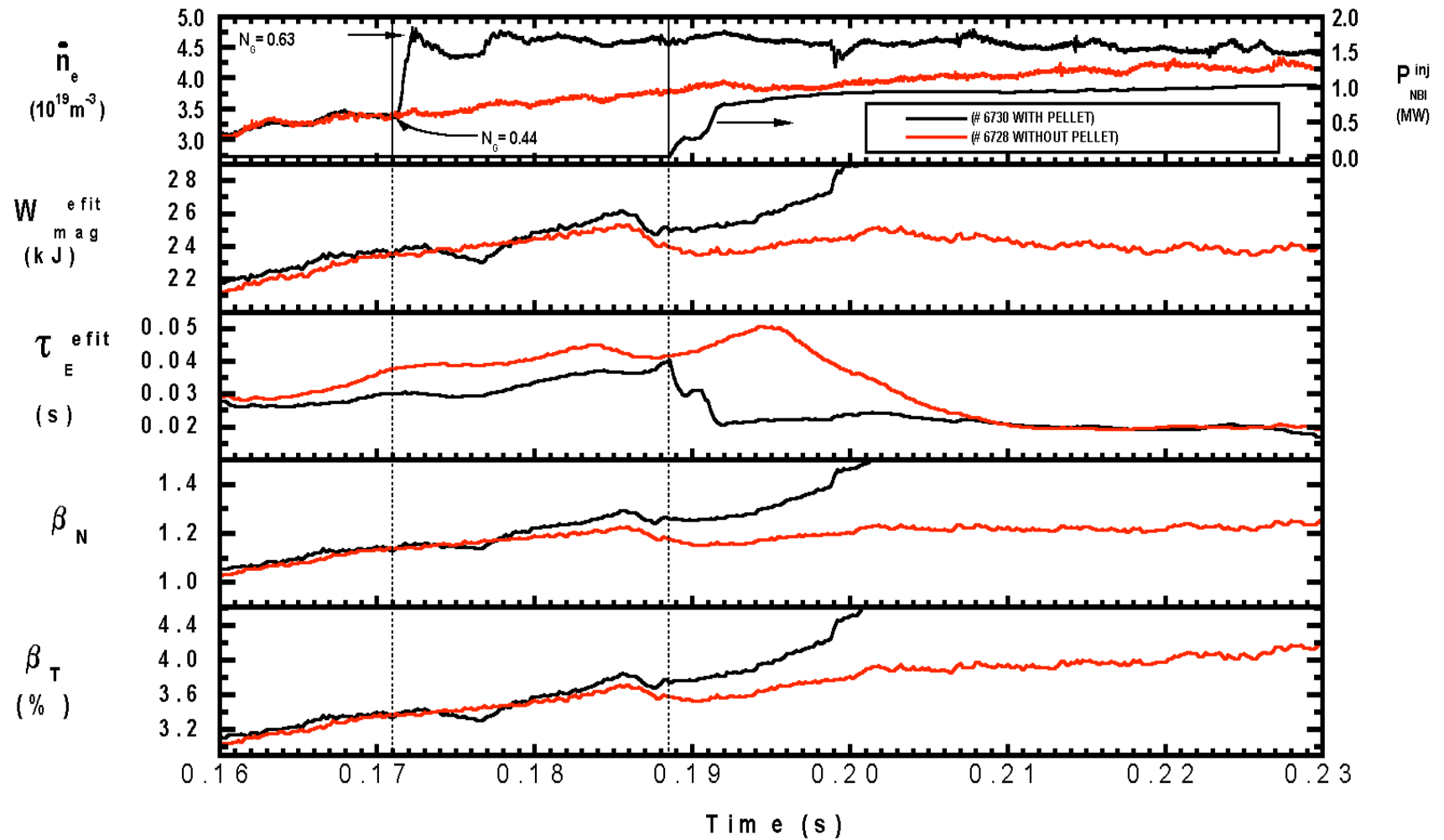


LFS Injection: longer density plateau ($\sim \square_E$)

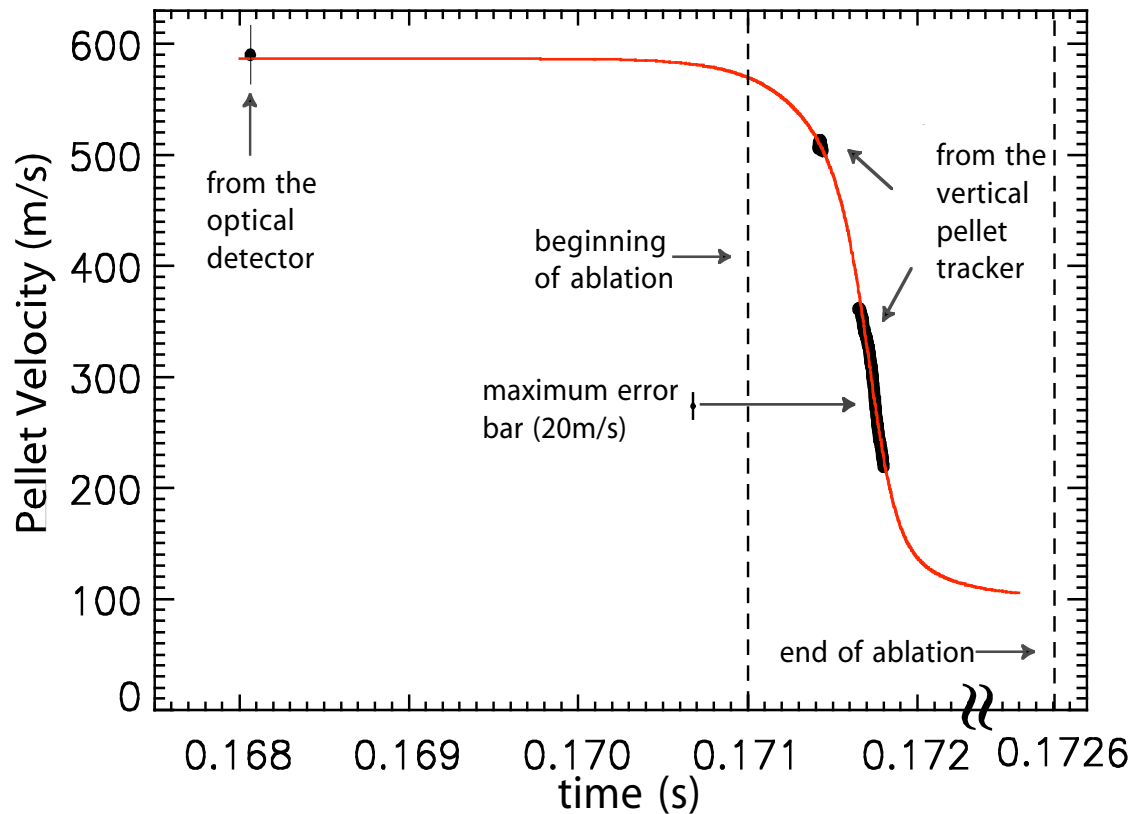
Vertical Injection: multi-pellet is favourable for longer plateau

LFS Injection: Ohmic (L-mode)/ NBI Regimes (L \square H)

#6730: $I_p \square 650\text{kA}$, $(1.0 \pm 0.3) \times 10^{20}$ atoms D, $V_p^{\text{det}} = 590 \pm 27$ m/s,



Pellet Velocity



$$\Delta t_{abl} = 1.60 \pm 0.11 \text{ms (D}_{\square} \text{ det.)}$$

$$\Delta t_{abl} = 1.56 \pm <0.31 \text{ms (HSV)}$$

$$\Delta \Delta p \equiv V_p^{det} \Delta t_{abl} \Delta 0.94 \pm 0.08 \text{m}$$

$$\Delta \Delta p \gg \Delta p^{CCD} = 0.46 \pm 0.02 \text{m}$$

ΔV_p really reduces!

More: $\int V_p dt = \Delta p^{CCD}$

ΔV_p slow down rate changes

How can this change in V_p slow down rate be interpreted based on LFS and HFS experiments?

Similar in START: $\Delta p^{CCD} = 0.29 \text{m}$ but $\Delta \Delta p \equiv V_p^{det} \Delta t_{abl} \Delta 0.51 \pm 0.06 \text{m}$

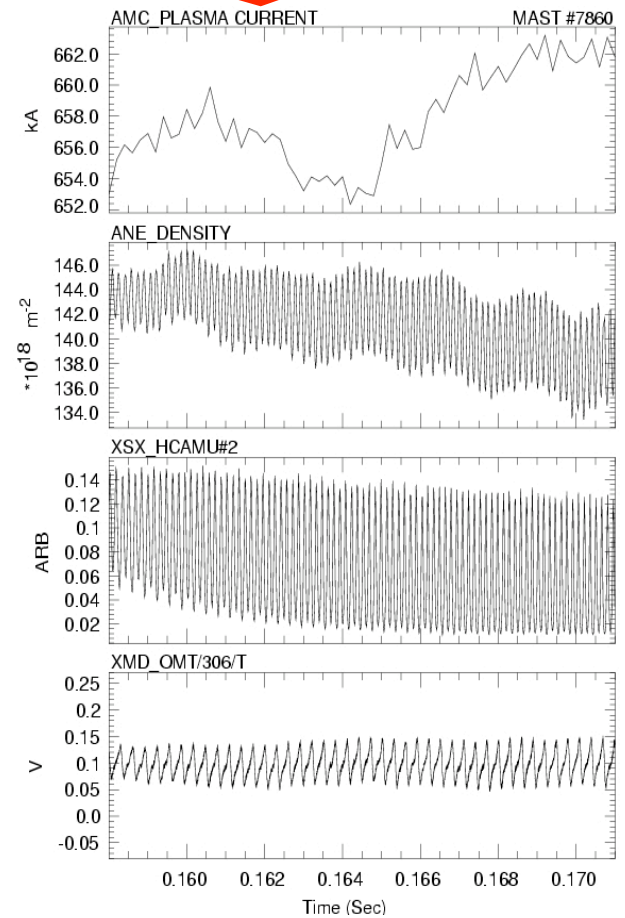
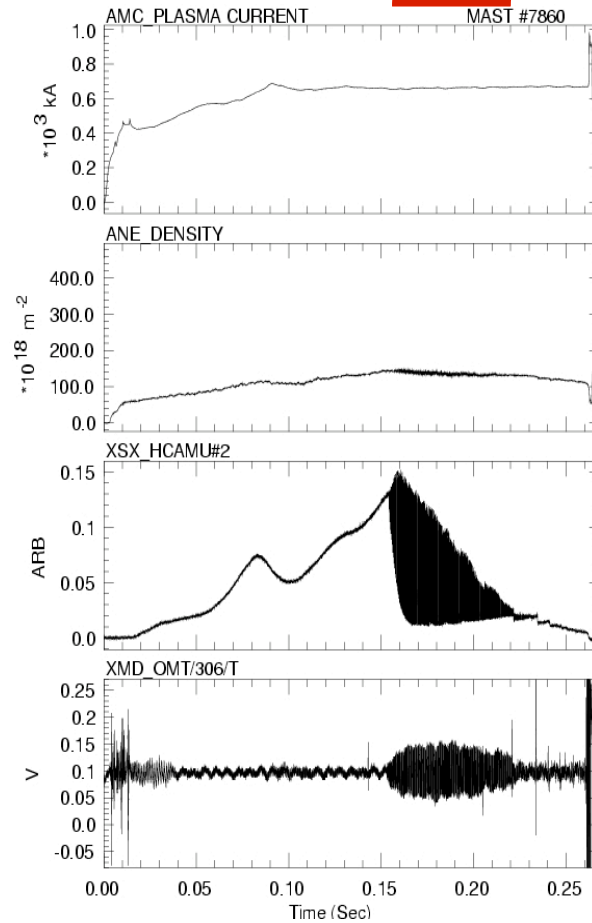
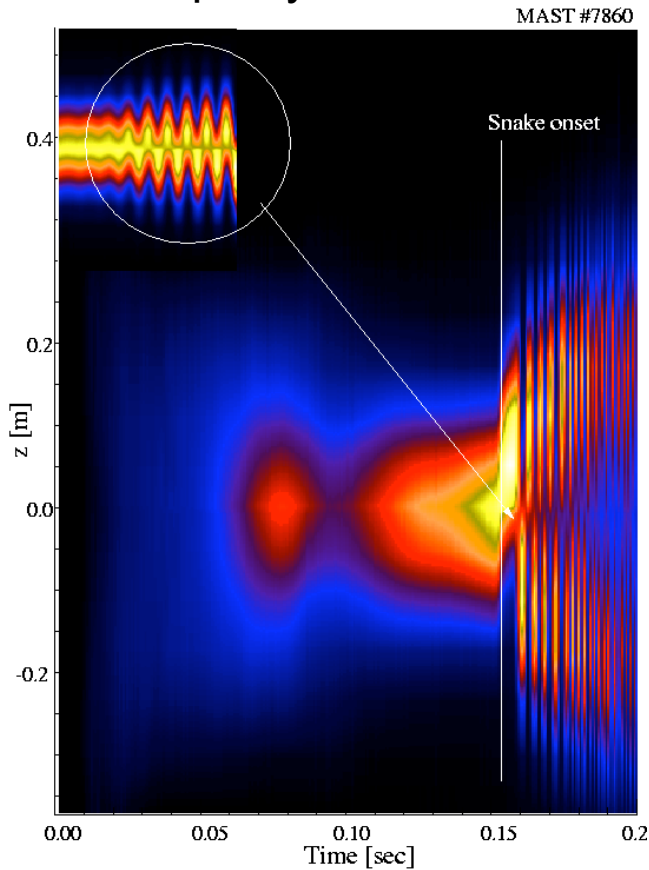
Does this dramatic slow down imposed any problem for core fuelling in ST reactor?

Spontaneous Snakes on MAST

Ian Lahane

Characteristics:

- Occur after a period of on axis impurity accumulation.

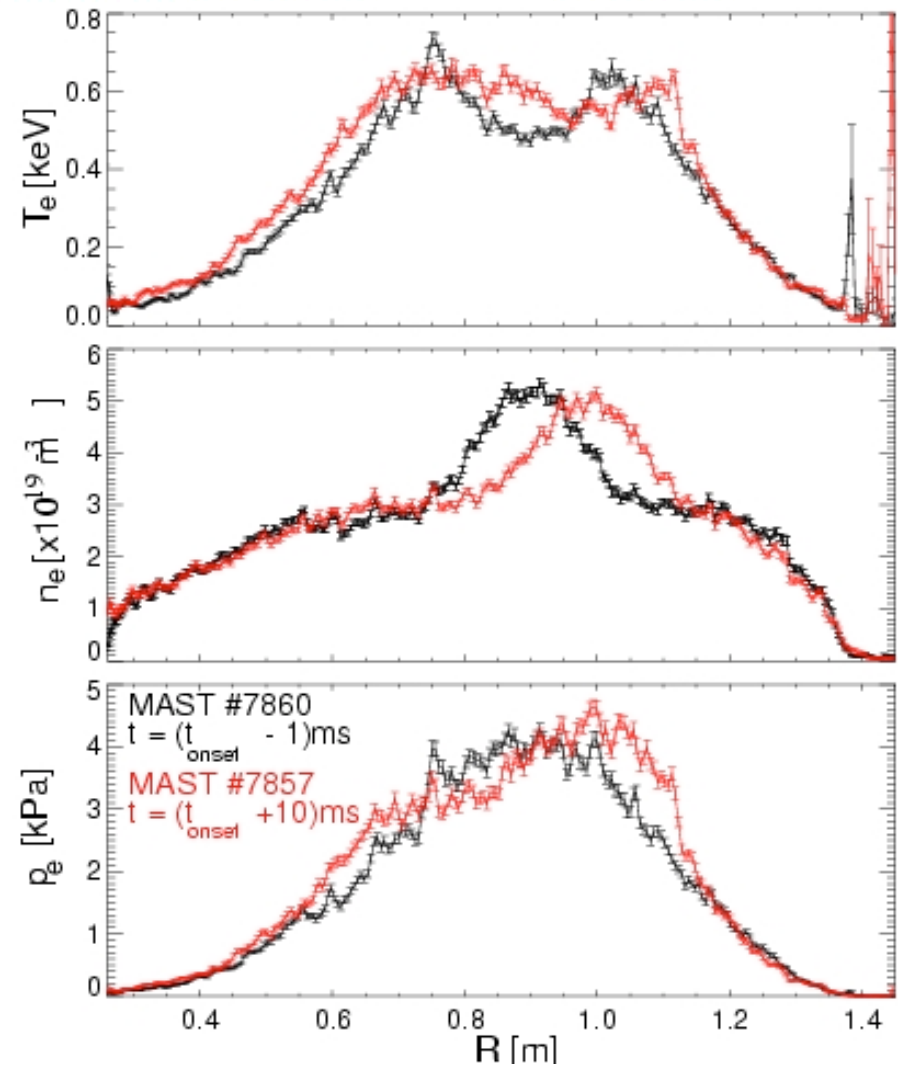
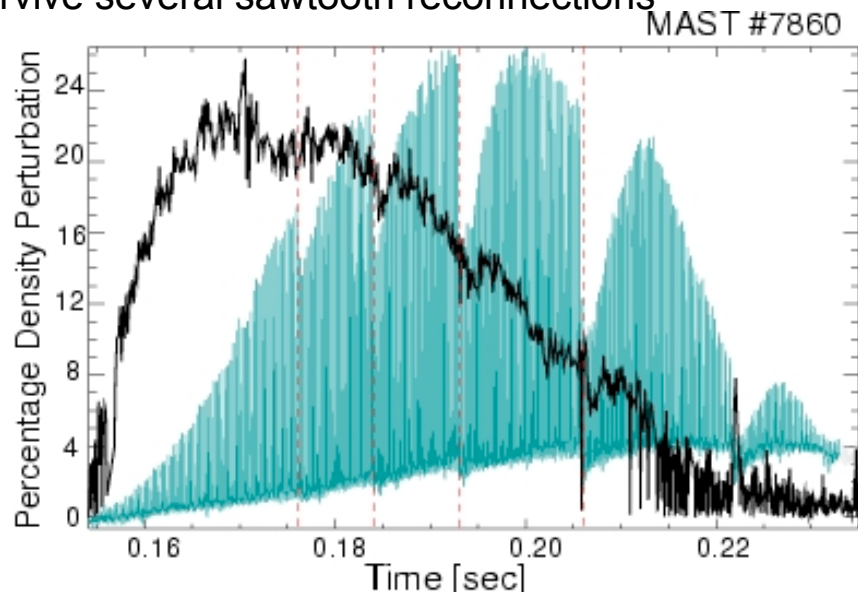




Effects on plasma conditions

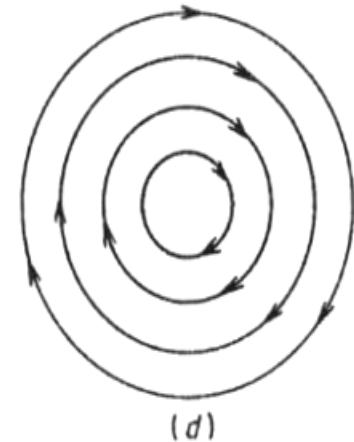
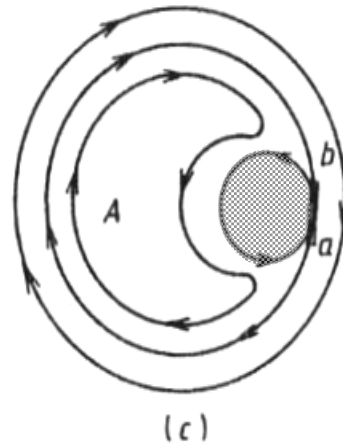
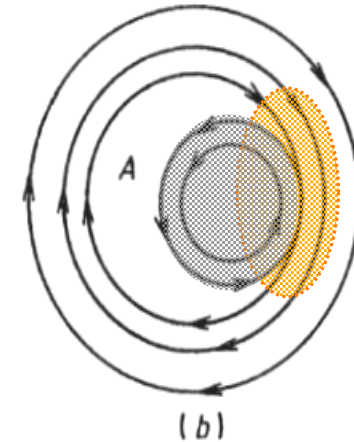
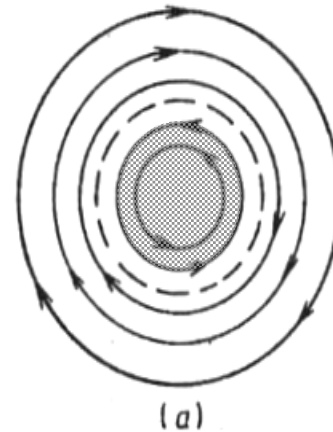
Characteristics:

- Strong perturbation of electron temperature and density ($\sim 20\%$).
- Electron temperature drop decays over tens of milliseconds.
- Density perturbations persist for time-scales up to order of observation times
- Survive several sawtooth reconnections



Onset Mechanism

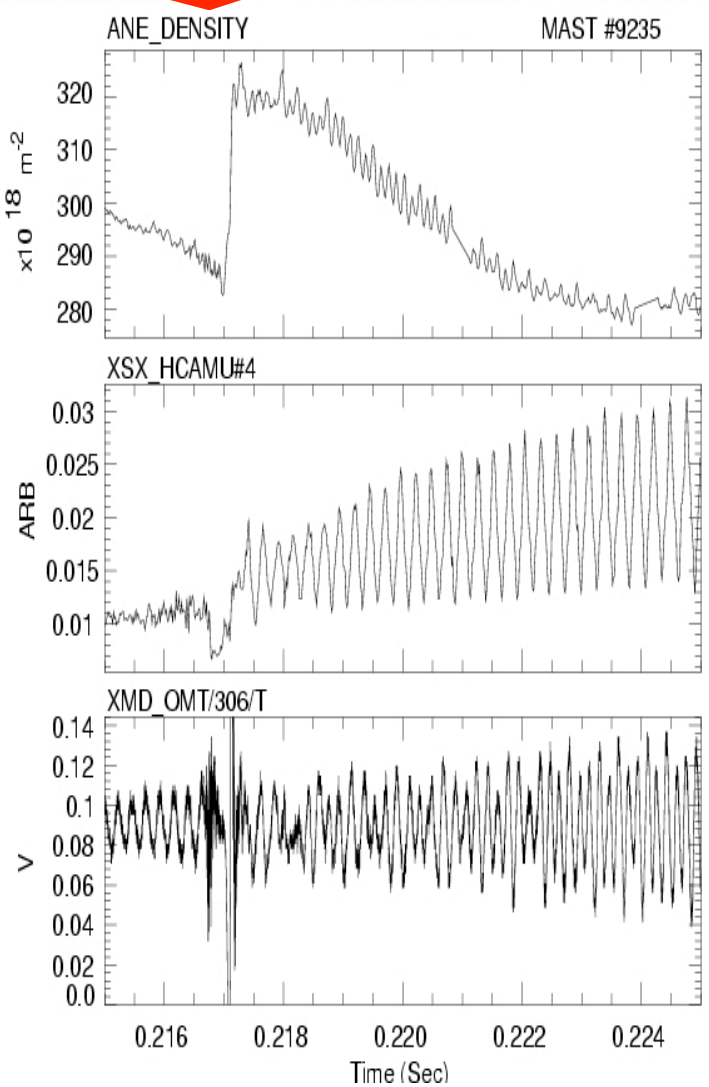
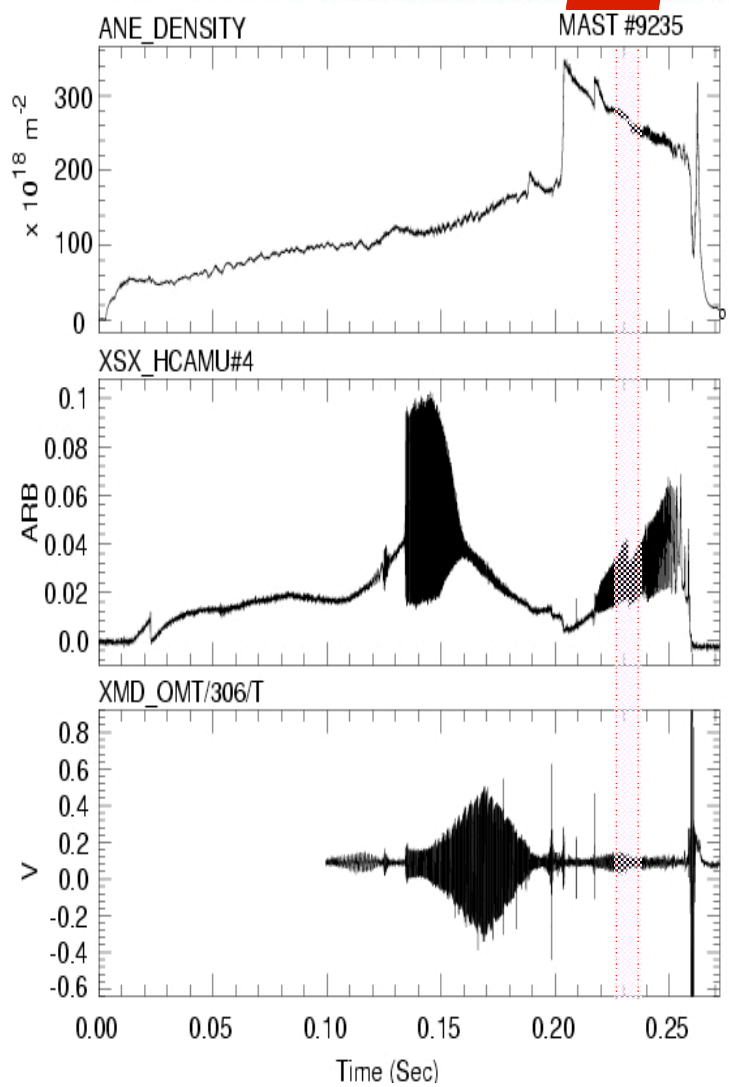
- Onset due to impurity accumulation in the core. $Z_{\text{eff}} \sim 4$ on axis.
- Good correlation between onset and decay of FeXVI impurity radiation during snake evolution.
- Core is displaced to form a helical radiating ring at the snake onset (b).
- Reconnection of $q < 1$ & $q > 1$ regions form an island which displaces the core, (b) & (c).



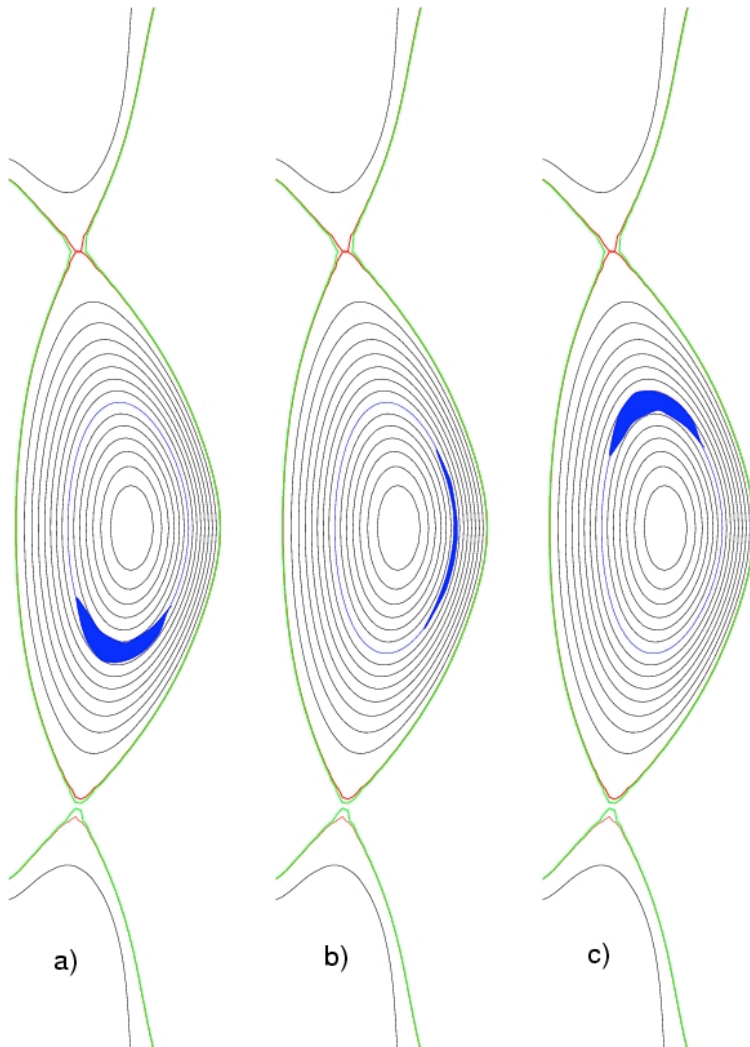


Pellet driven Snakes

- Pellet driven snakes are caused when high speed fuel pellets reach the $q=1$ surface.
- Pellet evaporates at each flux surface.
- On rational surfaces direct cooling is restricted to field lines intersecting the pellet trajectory.

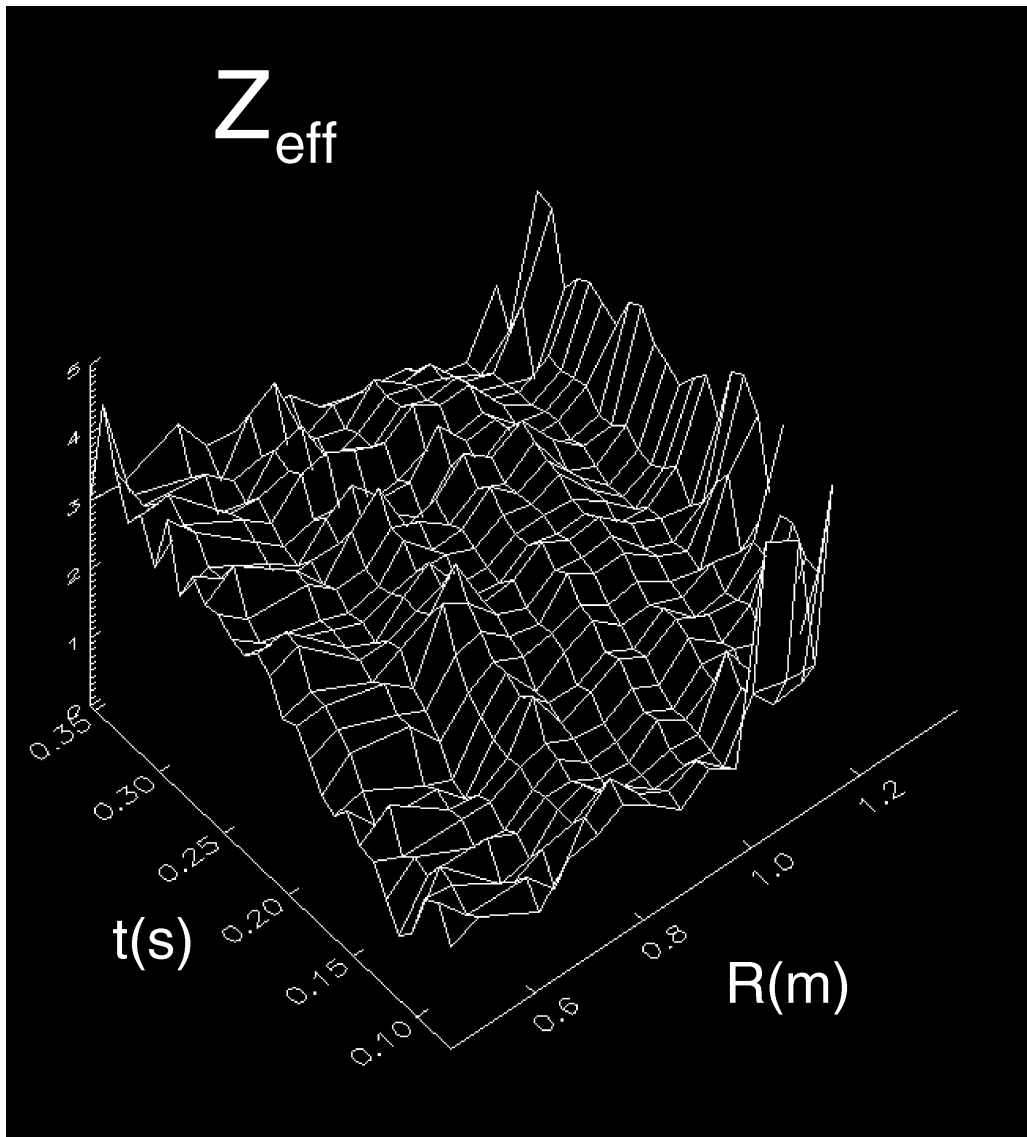


Snakes in magnetic islands



- Density perturbations for pellet driven snakes are measured to be of the same order as those of spontaneous snakes.
- Soft x-ray profiles show a significant difference in the profile evolution of the snake.
- This evolution is due to a radiation source within an island as opposed to the case of the spontaneous snakes.

Zeff profile example: reversed Ip, NBI-heated
Core Zeff increases with the line-average density from Zeff ~ 1.5 to ~ 3



- An imaging bremsstrahlung diagnostic has been commissioned on MAST to provide Z_{eff} profile measurements.

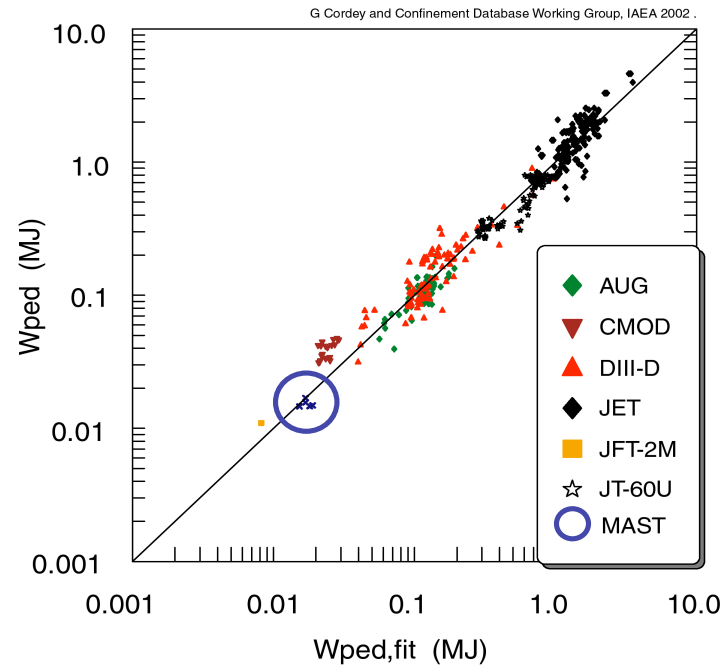
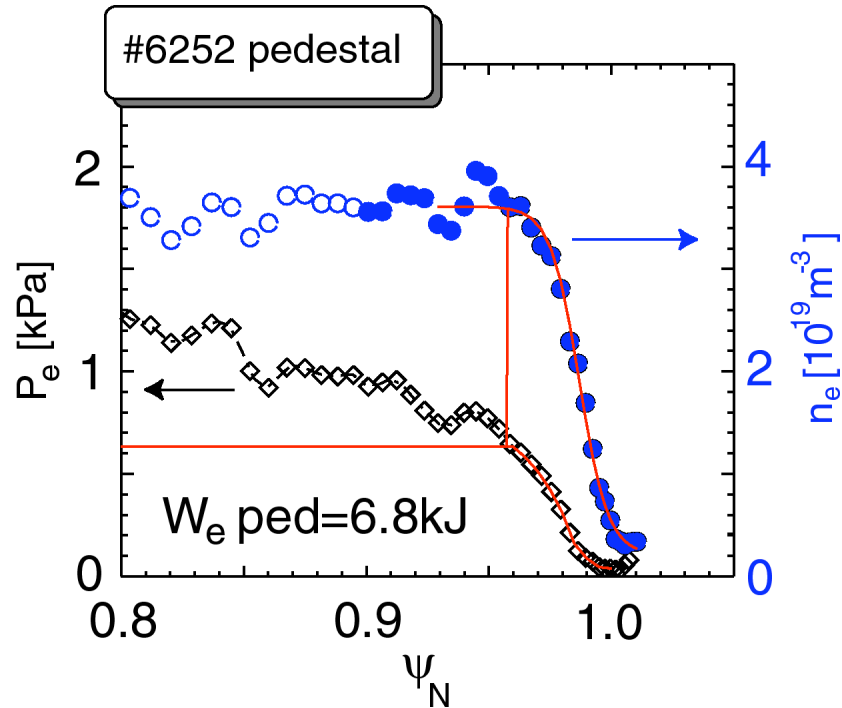
- Views one plasma cross-section (128x128 chords @200Hz or 256x256 chords @100Hz)

- System based on telecentric-optics, narrow band-pass filter and a frame-transfer CCD.

- MAST-plasma Z_{eff} values generally between 1-3

Ash Patel

H-mode Pedestal Scaling



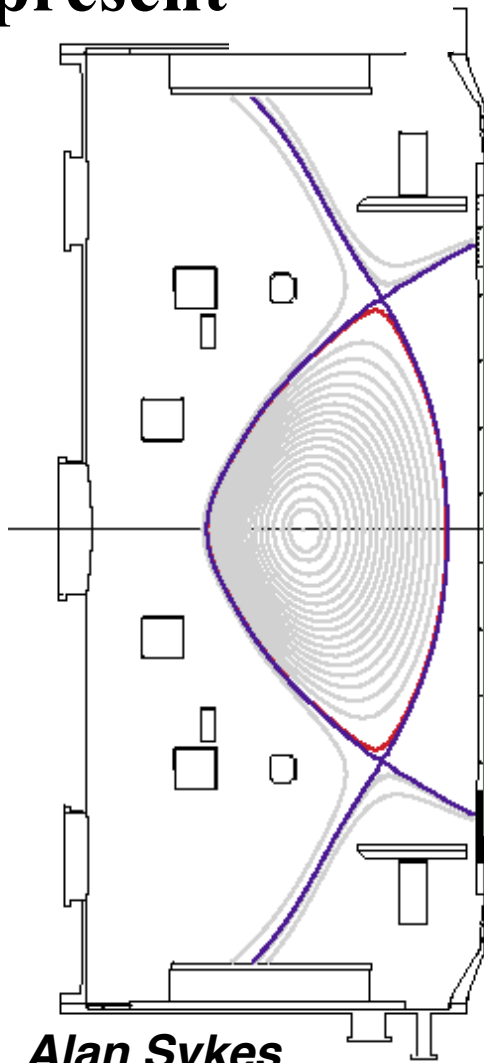
MAST pedestal energy calculated from full electron pressure profile.

Without MAST: $W_{ped,fit} \propto I^{1.4} R^{1.37} P^{0.50} n^{0.15} B^{0.32} a^{1.21} m^{0.2} (q_{95} / q_{cyl})^6$

With MAST: $W_{ped,fit} \propto I^{1.58} R^{1.08} P^{0.42} n^{0.08} B^{0.06} a^{1.81} m^{0.2} (q_{95} / q_{cyl})^{3.09}$

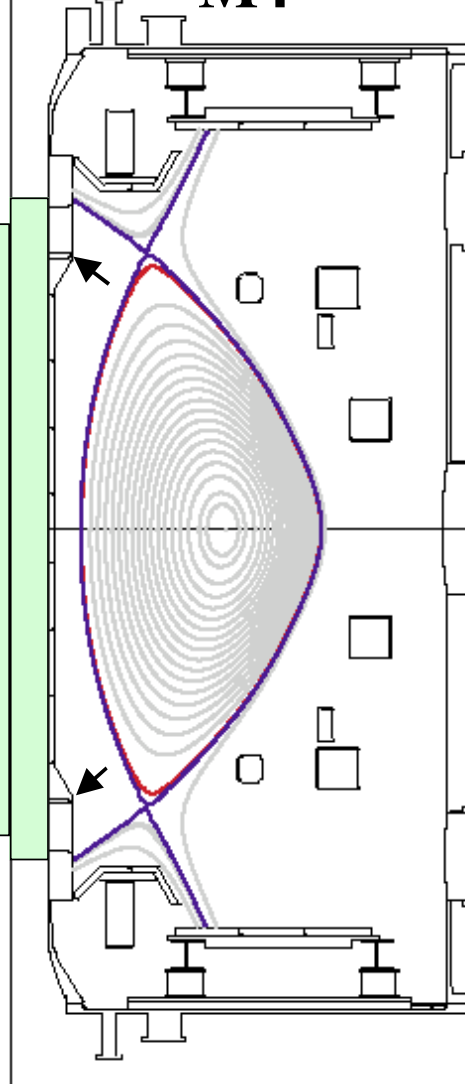
MAST Developments for M4

present



Alan Sykes

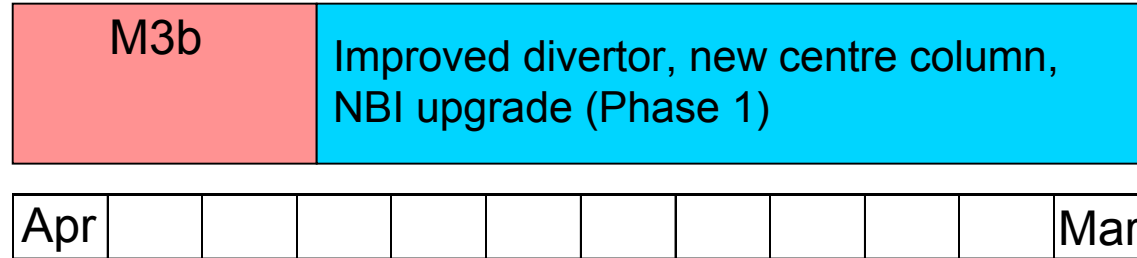
M4



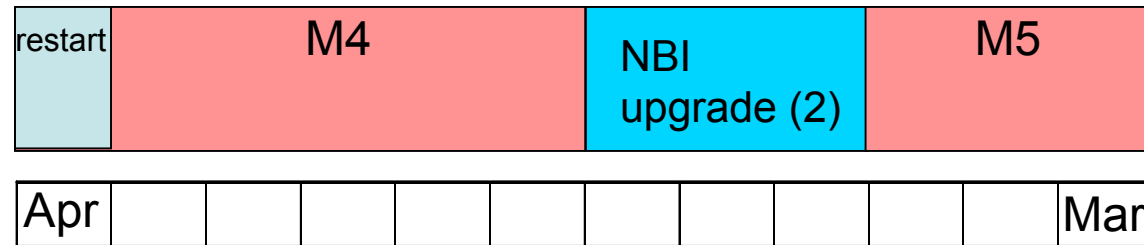
- Longer solenoid
- P2 coils raised by 10cm
- P2 current reversible to access higher elongation
- Shaped P2 armour
- Larger footprint for inner SOL strike points
- Controllable inner gas puff (arrowed)
- Higher power NBI
- Re-aligned EBW
- Digital control system
- Error field reduction

Operating Schedule

2003/04



**2004/05
(provisional)**



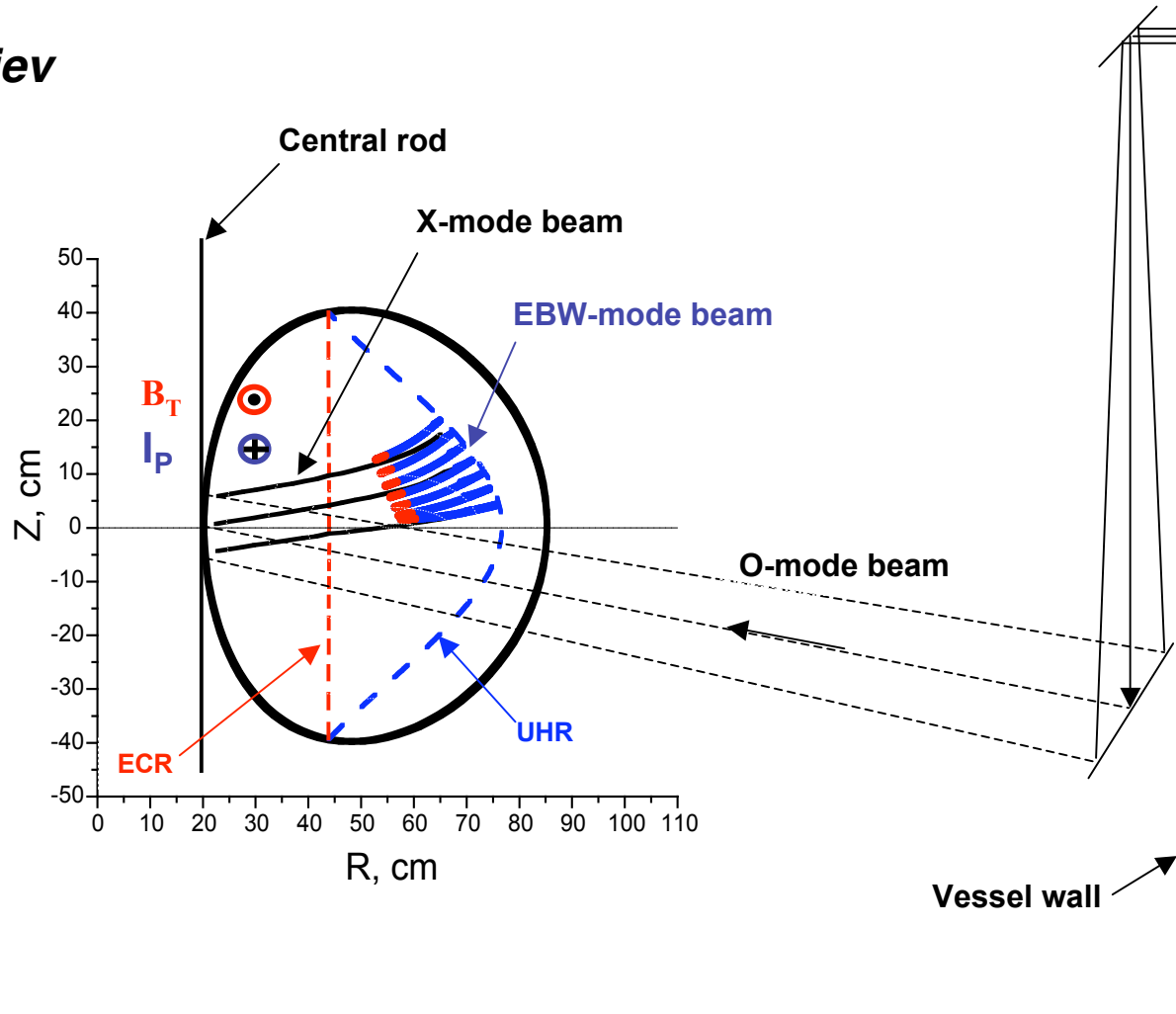
Operations



Engineering Break

EBWCD Start-up Scenario

A. Saveliev



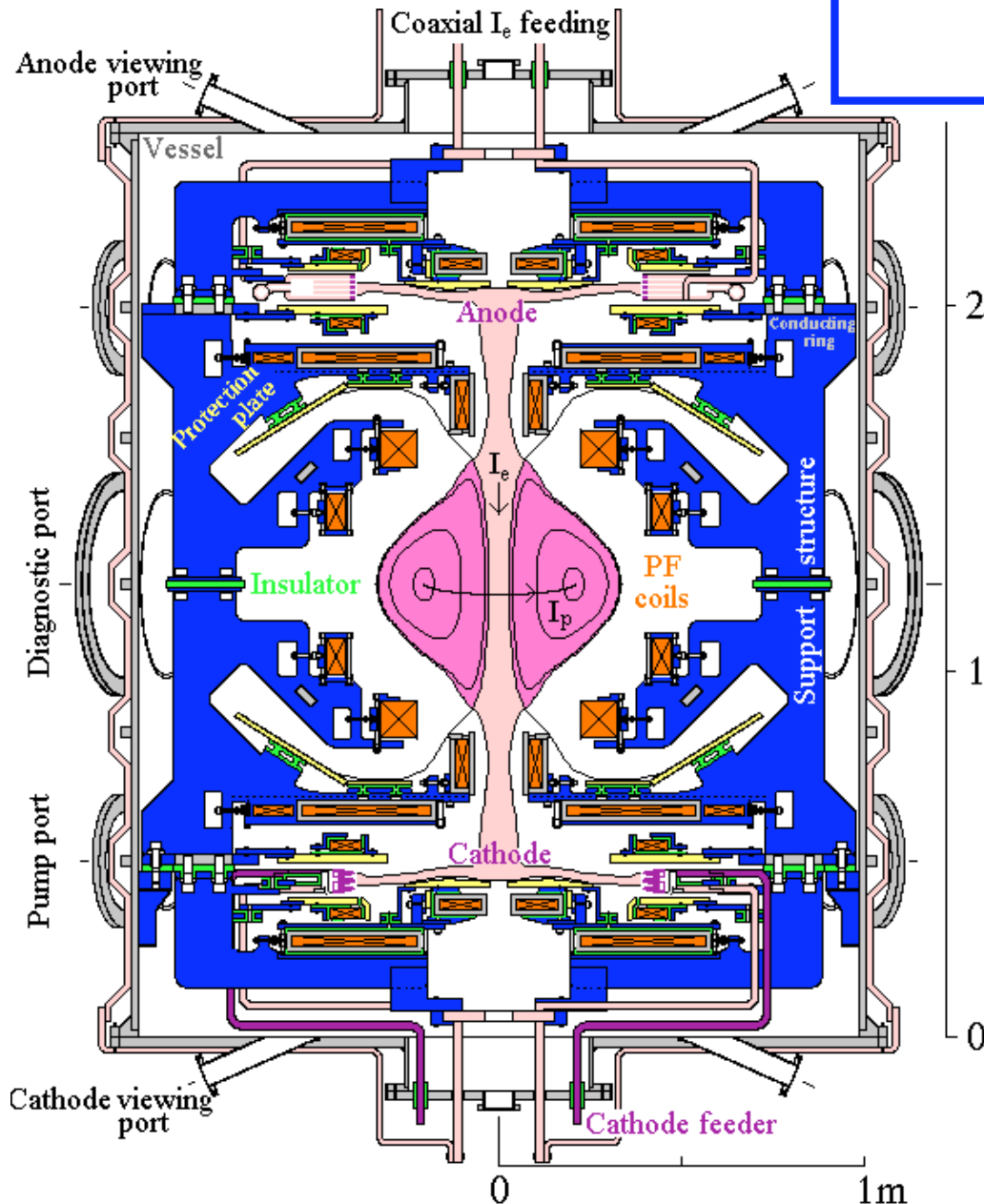
Schematic poloidal view of the EBW CD plasma initiation.

Assumptions/Open Questions

- Plasma density is lower than O-mode cut-off density.
For $f=28$ GHz, $n_e < 10^{19} \text{ m}^{-3}$.
- A grooved mirror-polariser must be incorporated into the central rod.
- Creation of the very initial stage of a discharge, when a seed current must be generated and an initial plasma equilibrium is formed needs additional studies and analysis.
- Can sufficient energy confinement be achieved to provide noticeable temperatures up to 1 keV in low density plasma sustained mainly by the EBW power?
- EBW driven current ramp-up will significantly change plasma equilibrium, which must influence the EBW current drive itself. Self-consistent simulation of the whole plasma evolution is desirable, but it is a very difficult task.

PROTO-SPHERA

Physics & Engineering Design



- ST diameter = 0.7m
- Toroidal plasma current

$$\underline{I_p = 240 \text{ kA}}$$

- Aspect ratio $A = 1.2$,
- Elongation $\kappa = 2.35$

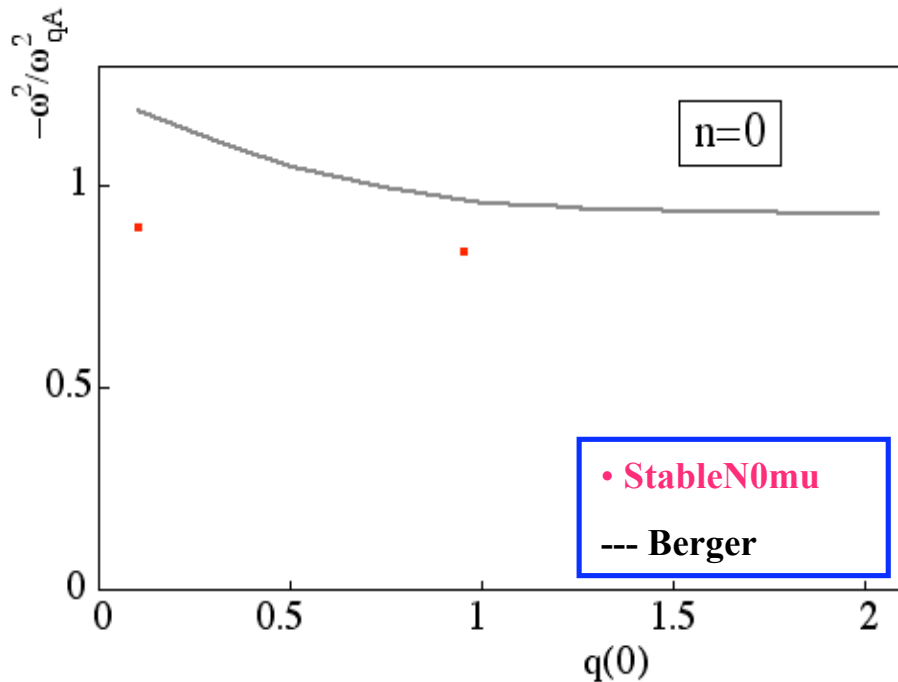
- Pinch current

$$\underline{I_e = 60 \text{ kA}}$$

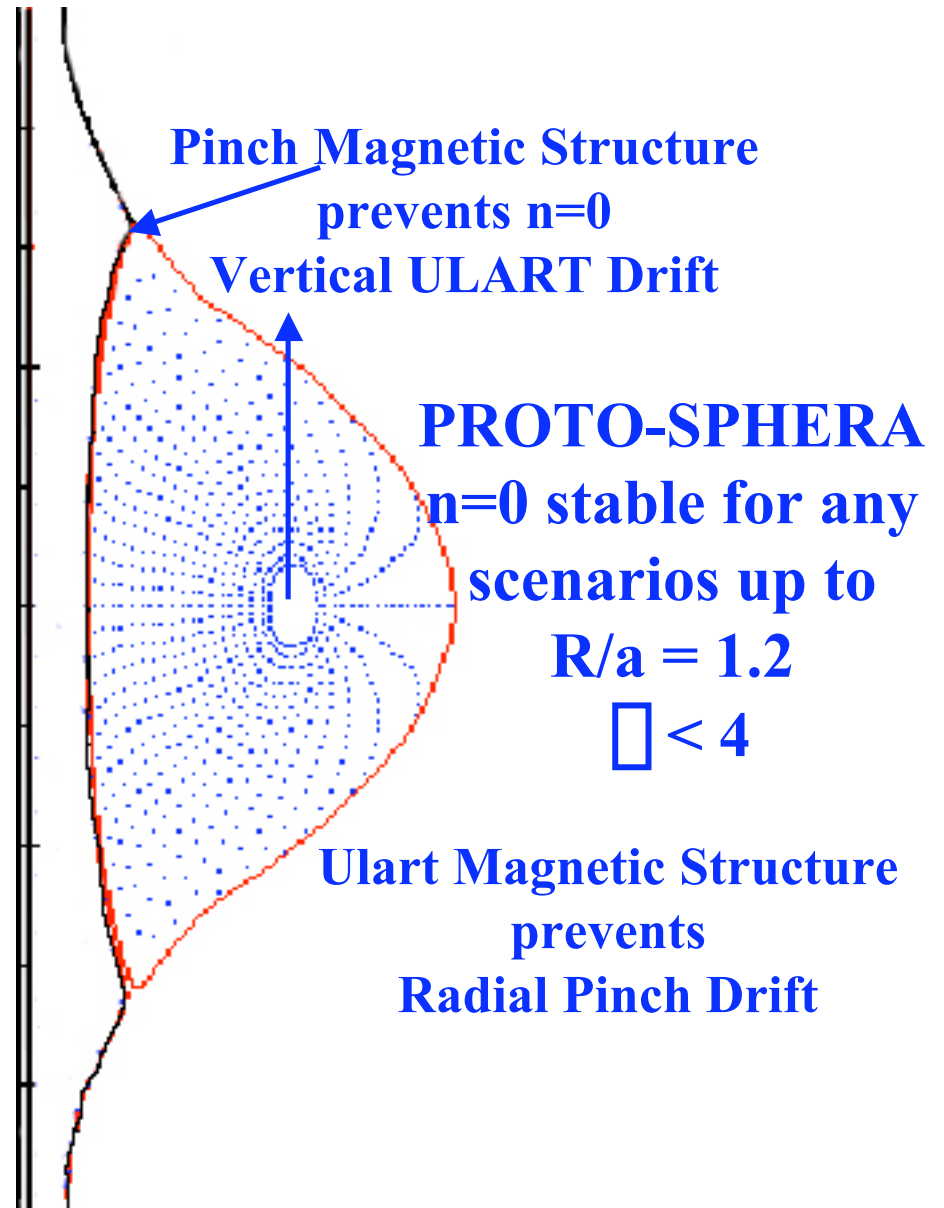
Complete engineering design:

- **Geometry of key components**
- **Estimation of the safety margins of stresses and temperatures**

Results STABLEN0mu Code: n=0



**Comparison of the
 instabilities growth rate for
 free boundary codes
 Mode numbers
 $n=0, m=[-15,+15]$.**



Some additional comments

Pegasus: Greg Garstka

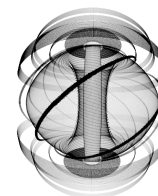
- **Completing extensive facility rebuild after a capacitor bank fire.**

Globus-M: Vasily Gusev

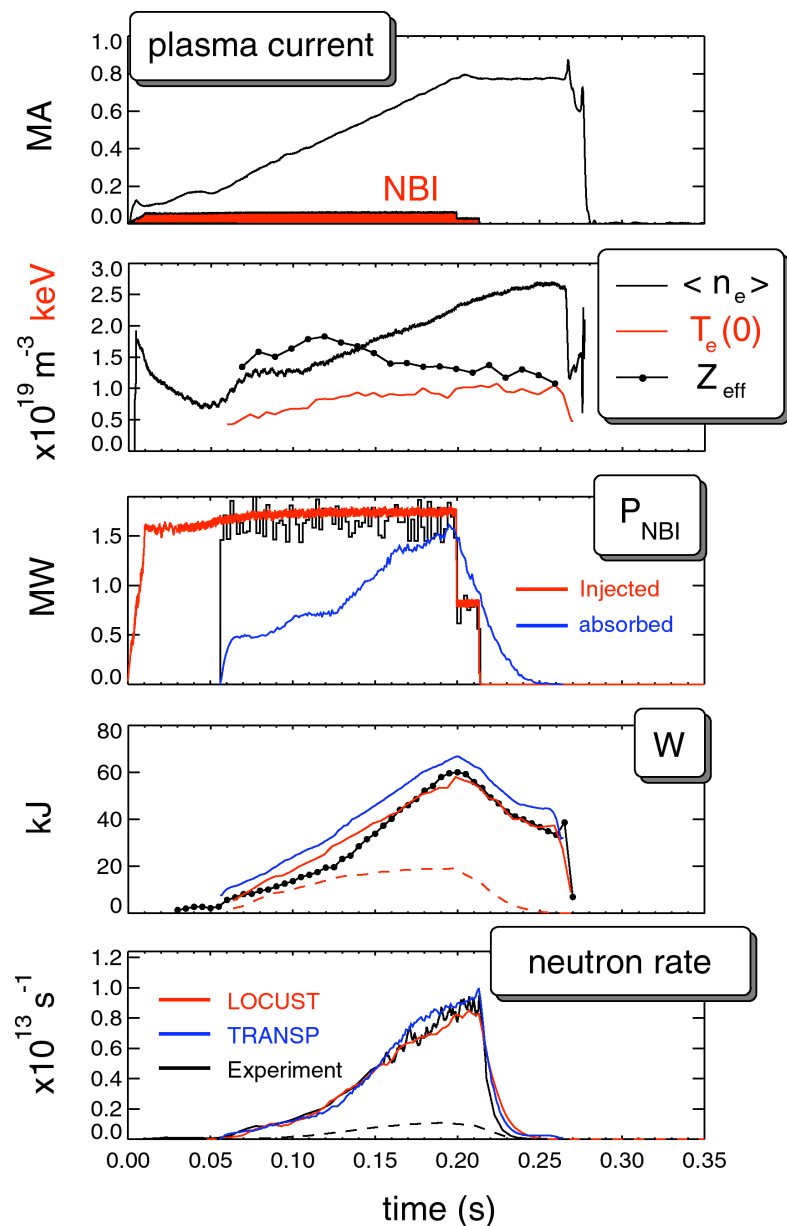
- **Globus-M is making progress in machine, diagnostic and plasma performance improvement**
- **Good performance OH discharge demonstrated signatures of auxiliary heating discharges: NTMs, bootstrap current, improved confinement**
- **In NBI auxiliary heating experiments, ion heating (but not electron) and plasma fuelling is demonstrated**
- **Unexpectedly high ion heating is observed in low power ICR heating experiments**

New Culham Director

- **The Culham staff are very upbeat about the appointment in September of Professor Sir Chris Llewellyn Smith FRS as the new Director of Culham. He is an enthusiast for fusion and has an impressive background in both the technical and political arenas**



Ion channel ITBs can be produced using CO-NBI



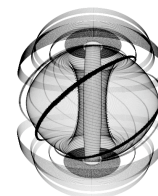
- Rapid I_p ramp with early NBI to maximise core rotation and inhibit current penetration

- Low density to maximise NBI penetration at $E=40keV$ and slow current penetration - $T_e(0)$ saturates at $\sim 1keV$, $Z_{eff}(0)$ reduces throughout the discharge

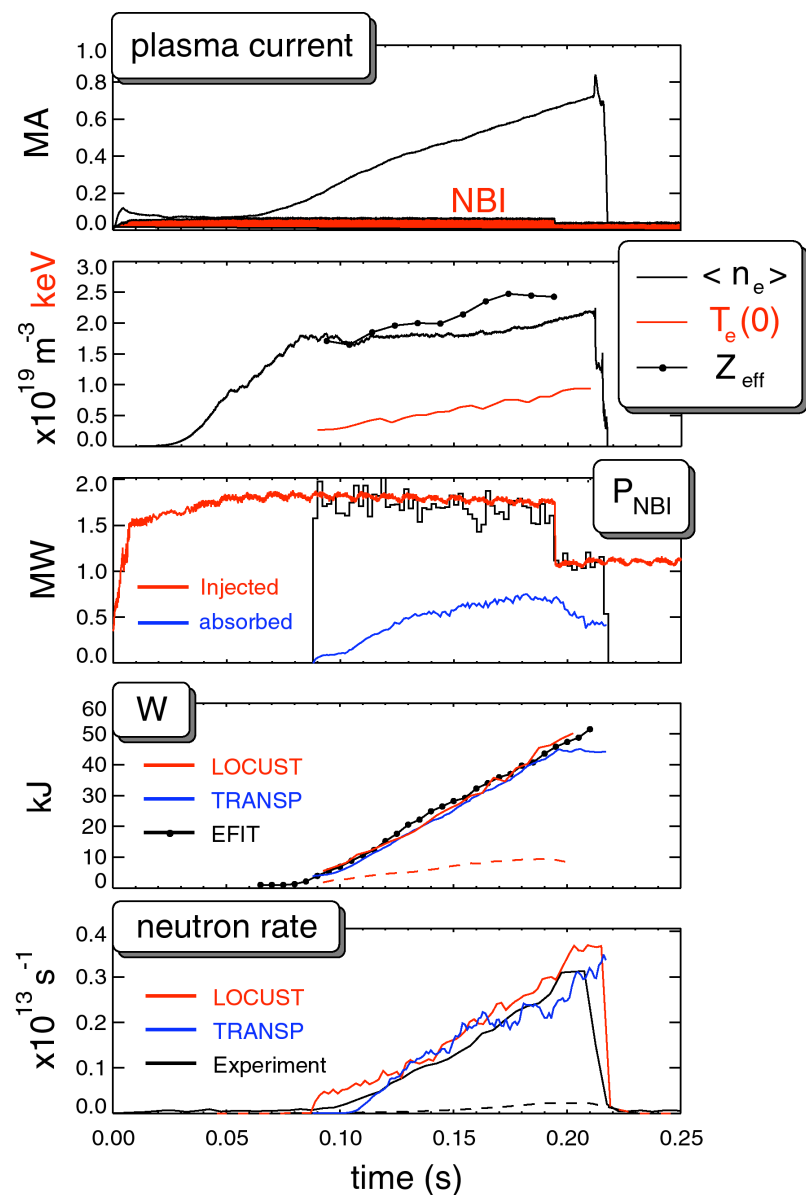
- $\sim 90\%$ of the NBI power is absorbed by the plasma at 200ms

- Stored energy from TRANSP and LOCUST are in good agreement with EFIT

- LOCUST and TRANSP neutron rates in excellent agreement with experimental data



Electron channel ITBs can be produced using Counter-NBI



Rapid I_p ramp with early NBI to maximise core rotation and inhibit current penetration

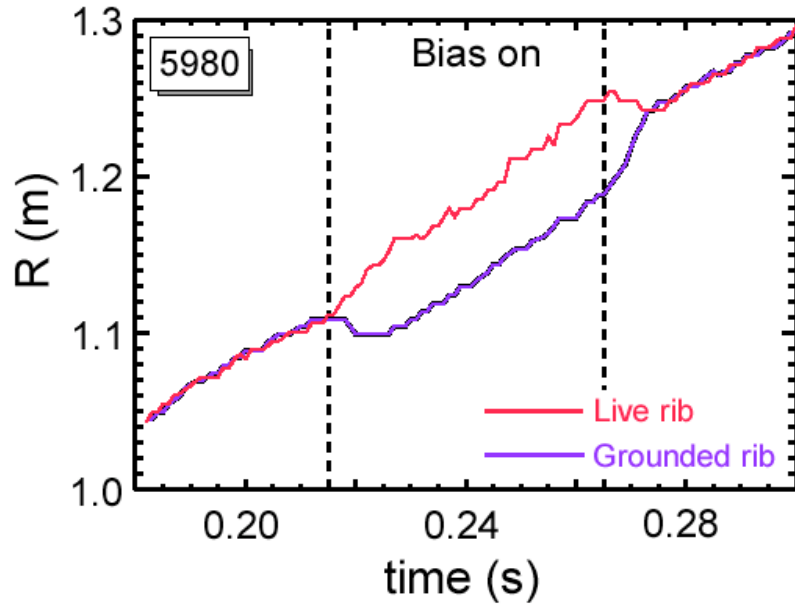
Low density to maximise NBI penetration at $E=40\text{keV}$ and slow current penetration - $T_e(0)$ rises linearly, $Z_{eff}(0)$ tolerable, Z_{eff} profile \sim flat.

TRANSP and LOCUST indicate that $<50\%$ of the NBI power is absorbed by the plasma

Stored energy from TRANSP and LOCUST agrees well with magnetics

W comparable to Co-NBI even though neutron rate down by factor 1/3 (in good agreement with modelling).

Biasing results in strike-point motion point



- **Strike-points shift in opposite directions during biasing**
- **Direction reverses with toroidal field reversal**
- **Agrees with theory in magnitude and direction**

